Willmore-type regularization of mean curvature flow in the presence of a non-convex anisotropy.
The graph setting: analysis of the stationary case and numerics for the evolution problem.

Paola Pozzi
Universität Duisburg-Essen
Fakultät für Mathematik
Forsthausweg 2
47057 Duisburg, Germany
paola.pozzi@uni-due.de

Philipp Reiter
Abteilung für Angewandte Mathematik
Albert-Ludwigs-Universität Freiburg
Hermann-Herder-Straße 10
79104 Freiburg i. Br., Germany
reiter@mathematik.uni-freiburg.de

January 20, 2012

Abstract

In this paper we investigate the motion of one dimensional graphs under anisotropic non-convex mean curvature flow regularized via a Willmore term. Aiming at understanding the evolution problem when we let the regularization parameter tend to zero, we first present rigorous analytical results for the stationary case. Subsequently we discuss the time dependent problem focussing mainly on numerical simulations. We discretize by finite elements,provide a semi implicit scheme and a number of numerical experiments.

MSC2010: 35G31, 65M60, 35Q99.

Contents

1 Introduction

In recent years many authors have studied curvature-dependent interface motion under several kinds of interfacial energies. In applications where a planar sharp phase-interface is modelled, one is typically interested in evolution equations of type

$$b(\theta)V = \big(f(\theta) + f''(\theta)\big)\varkappa - F, \tag{1.1}$$

relating the normal velocity V to the curvature $\varkappa$ (see Angenent and Gurtin [1] and Gurtin's monograph [16]). Here θ stands for the angle of the interface normal to some fixed axis, b is a positive map that characterizes the kinetics and measures the drag opposing interfacial motion, f is the interfacial energy, and F is the difference in bulk energy between phases.

There are numerous extensions and generalizations of (1.1). In fact, it is a special case of a general geometric evolution equation $V = \Phi(x, \nu, \varkappa)$ where the normal velocity depends on position, normal direction, and curvature. Besides the well known motion by mean curvature ($V = \varkappa$) and all its anisotropic variants, many physical processes are naturally associated to evolution laws of this kind, see for instance Deckelnick, Dziuk, and Elliott [12], Bellettini [2] and references given in there.

It is well known that material scientists also use energies for which $(f + f'')$ is negative on some intervals (see for instance references given in Gurtin and Jabbour [17]). The problem with this approach is that the associated evolution equation becomes forward-backward parabolic. To deal with the inherent instability one usually adds a higher order term to the surface energy. The regularization proposed by Angenent and Gurtin [1] and subsequently studied by Di Carlo, Gurtin, and Podio-Guidugli [13] has the form

$$b(\theta)V = \big(f(\theta) + f''(\theta)\big)\varkappa - F - \varepsilon^2\left(\varkappa_{ss} + \tfrac{1}{2}\varkappa^3\right) \qquad (s = \text{arc-length}) \tag{1.1$_\varepsilon$}$$

with $\varepsilon > 0$ small, and leads to a fourth oder evolution equation (cf. Spencer [22] and references therein for an overview over this approach).

In this paper we start an investigation of motion of one dimensional graphs under anisotropic non-convex mean curvature flow regularized via a Willmore term. More

precisely we consider the L^2-gradient flow of the energy

$$E_\varepsilon : u \mapsto \int_{\text{graph } u} \gamma(\nu)\,\mathrm{d}A + \varepsilon^2 \int_{\text{graph } u} \varkappa^2\,\mathrm{d}A, \qquad \varepsilon > 0, \tag{1.2}$$

where $\varkappa$ denotes the curvature of the graph of u, ν its unit normal, and γ is non-convex. In other words we study the functional

$$E_\varepsilon : u \mapsto \int_0^1 \left(g(u_x(x)) + \varepsilon^2 \frac{u_{xx}(x)^2}{(1+u_x(x)^2)^{5/2}} \right) \mathrm{d}x, \tag{4.1}$$

where $g(y) := \gamma(y,-1)$. Note that with $\nu = (\cos\theta, \sin\theta)$ and $\gamma(\nu) = f(\theta)$ one easily recovers the evolution equation (1.1_ε) (with $F \equiv 0$ and $b \equiv 1$) and that the non-convexity of γ is related to the negative sign of $(f + f'')$ (see Section 5, in particular Remark 5.1). The curvature-dependent regularization term in Equation (4.1), which is analytically far more complicated than $\varepsilon^2 u_{xx}^2$, is motivated in Di Carlo, Gurtin, and Podio-Guidugli [13], where a derivation of (1.1_ε) is discussed.

The problem of anisotropic flows with curvature regularization has already been considered from a numerical point of view in Haußer and Voigt [19] (motion of curves in the plane, parametric setting) and in Burger, Haußer, Stöcker, and Voigt [7] (level-set approach). Furthermore very interesting numerical experiments with non-convex functionals are presented in Fierro, Goglione, and Paolini [15]: in particular the simulations indicate that in general a non-convex anisotropy and its convexification can give rise to different evolutions (in [15] the original equations are approximated by means of a full discretization, which is always well-posed for fixed values of the discretization parameters).

The fourth order evolution equation associated with (4.1) takes the form

$$\frac{u_t}{\sqrt{1+u_x^2}} = g''(u_x)u_{xx} - \frac{\varepsilon^2}{(1+u_x^2)^{1/2}} \left(2\frac{u_{xxxx}}{(1+u_x^2)^2} - 20\frac{u_x u_{xx} u_{xxx}}{(1+u_x^2)^3} + \frac{u_{xx}^3}{(1+u_x^2)^4}(30u_x^2 - 5) \right) \tag{5.2}$$

plus boundary conditions.

Our long term plan is to try to understand (5.2) in the limit $\varepsilon \searrow 0$. This is far from being a trivial task as also pointed out in Bellettini, Fusco, and Guglielmi [4] where a similar one dimensional problem is studied from an analytical and numerical point of view (there the authors consider the gradient flow associated to the functional $\int_I \phi(u_x)\,\mathrm{d}x + \varepsilon^2 \int_I u_{xx}^2\,\mathrm{d}x$ with non-convex ϕ; see also Bellettini and Fusco [3] and references therein). Our hope is that the physical consistency of the model we have chosen will strongly help in the derivation of a meaningful notion of weak solution for (5.2) when ε tends to zero. For the stationary case Spencer [22] studies the effect of the regularization on the equilibrium shape.

In this work we present first steps in this direction: we start by analyzing the stationary problem for the functional E_0 (cf. (2.4)) defined on

$$\mathscr{C}_{\alpha,\beta} := \left\{ u \in H^{1,1}(0,1) \,\middle|\, u(0) = \alpha, u(1) = \beta \right\}, \qquad \alpha, \beta \in \mathbb{R}, \tag{2.3}$$

(Section 3) as well as for $E_\varepsilon(u)$, $u \in \mathscr{C}_{\alpha,\beta} \cap H^{2,2}(0,1)$ (Section 4). Using some ideas of Carr, Gurtin, and Slemrod [9] and further simple but beautiful geometric arguments we derive a number of properties for the minimizers of E_ε, $0 < \varepsilon \ll 1$. Let us here mention that for a situation as depicted in Figure 1 with $\omega = \beta - \alpha \in (1,2)$ we show that

(i) there exist minimizers of the form

$$\left(u_\varepsilon : x \mapsto \alpha + \int_0^x v_\varepsilon(\xi)\,\mathrm{d}\xi\right) \in \mathscr{C}_{\alpha,\beta} \cap H^{2,2}(0,1) \tag{4.3}$$

where v_ε is a strictly monotone map with image lying in a fixed bounded interval $[z_\omega^-, z_\omega^+]$ determined by g,

(ii) minimizers u_ε of E_ε in $\mathscr{C}_{\alpha,\beta} \cap H^{2,2}(0,1)$ satisfy the uniform bound $\|u_\varepsilon\|_{H^{1,\infty}(0,1)} \leq C$, where C does not depend on ε, and

(iii) a sequence of convex minimizers u_ε converges to $\bar{\bar{u}}$ in $H^{1,p}(0,1)$ for $p \in [1,\infty)$, where $\bar{\bar{u}}(x) = \alpha + \int_0^x \bar{\bar{v}}(\xi)\,\mathrm{d}\xi$ and $\bar{\bar{v}}$ is an increasing step function taking only two values, namely

$$\bar{\bar{v}} := z_\omega^- \chi_{(-\infty,x_*)} + z_\omega^+ \chi_{(x_*,\infty)} \qquad \text{where} \qquad z_\omega^- x_* + z_\omega^+(1-x_*) \equiv \omega \tag{4.11}$$

and $\chi_\cdot$ is the characteristic function.

(More details can be found in Theorem 4.1 and Corollary 4.2.)

The method of proof makes clear in which way the regularization term selects some of the minimizers for E_0. One could obtain similar statements also by using Gamma-convergence analysis but it turns out that in this case a direct analysis is less complicated and has in our opinion the advantage to be very transparent.

In the second part of this paper we tackle the evolution problem. After a derivation of the classical formulation of the flow in Section 5 we shortly discuss the difficulties that arise when we analyse the evolution in the limit $\varepsilon \searrow 0$ (Section 6). In order to get an idea of what should be expected, we discretize the problem by the finite element method (Section 8), we provide a semi-implicit scheme (as opposed to Bellettini et al. [4] who employ a Radau-IIA Runge-Kutta method) and a number of numerical simulations (Subsection 9.3). The choice of numerical tests pays particular attention to the phenomenon of (ε-dependent) microstructures formation ("wrinkles"), that is observed during the first stage of the evolution and that is theoretically reviewed in Section 7.

Acknowledgements. We are greatly indebted to C. M. Elliott for suggesting the topic and for several very stimulating discussions. Furthermore we would like to thank G. Dziuk for many helpful conversations and the DFG Transregional Collaborative Research Centre SFB TR 71 for its generous financial support.

2 Preliminaries and notation

We will consider anisotropy functions $\gamma : \mathbb{R}^2 \to [0,\infty)$, that are Lipschitz continuous, positive, and positively homogeneous of degree one, i. e.

(L)	$\gamma \in C^{0,1}(\mathbb{R}^2)$,	
(P)	$\gamma(p) > 0$	for $p \neq 0$,
(H)	$\gamma(\lambda p) = \lvert\lambda\rvert\,\gamma(p)$	for $\lambda \in \mathbb{R}$, $p \in \mathbb{R}^2$.

Conditions (H) and (L) ensure the existence of a global Lipschitz constant for γ. Note that the above assumptions on the anisotropy function γ allow for a wide class of Frank diagrams

$$\mathcal{F}_\gamma := \left\{ p \in \mathbb{R}^2 \,\middle|\, \gamma(p) \le 1 \right\}. \tag{2.1}$$

Indeed, these can be non-convex or crystalline. The isotropic case is recovered by choosing $\gamma(p) = |p|$.

In what follows we will be concerned with the study of the functional

$$E_0 : u \mapsto \int_{\operatorname{graph} u} \gamma(\nu)\,\mathrm{d}A, \qquad u \in \mathscr{C}_{\alpha,\beta}, \tag{2.2}$$

where ν is the (Euclidean) normal to the graph of u,

$$\mathscr{C}_{\alpha,\beta} := \left\{ u \in H^{1,1}(0,1) \,\middle|\, u(0) = \alpha, u(1) = \beta \right\}, \qquad \alpha,\beta \in \mathbb{R}, \tag{2.3}$$

and γ is in general non-convex. Since $\nu(x,u(x)) = \frac{(u_x(x),-1)}{\sqrt{1+u_x(x)^2}}$, we can write

$$E_0(u) \overset{(2.2)}{=} \int_{\operatorname{graph} u} \gamma(\nu)\,\mathrm{d}A \overset{(H)}{=} \int_0^1 g(u_x(x))\,\mathrm{d}x, \tag{2.4}$$

where

$$\left(g : y \mapsto \gamma(y,-1)\right) \in C^{0,1}(\mathbb{R},(0,\infty)). \tag{2.5}$$

Some examples of functions g and related Frank diagrams (2.1) are given in Figures 1, 2, and 4. Moreover from

$$0 < c_0 := \min_{\tau\in S^1} \gamma(\tau) \le \gamma(\nu) \le \max_{\tau\in S^1} \gamma(\tau) =: c^0 < \infty$$

we infer from (H) that

$$c_0 \le c_0 \sqrt{1+u_x(x)^2} \le g(u_x(x)) \le c^0 \sqrt{1+u_x(x)^2},$$

thus $E_0(u)$ is well-defined. Moreover we deduce that g grows linearly at infinity and has at least one minimum point. We set

$$g^\infty := \gamma(\pm 1, 0) \overset{(H)}{=} \lim_{y\to\pm\infty} \frac{g(y)}{|y|}.$$

Sometimes it is convenient to express the Frank diagram though a 2π-periodic radial function $\varrho : \mathbb{R}/2\pi\mathbb{Z} \to (0,\infty)$ via

$$\mathcal{F}_\gamma = \left\{ \lambda \begin{pmatrix} \cos\varphi \\ \sin\varphi \end{pmatrix} \,\middle|\, \varphi \in [0,2\pi], \lambda \in [0,\varrho(\varphi)] \right\}.$$

The maps γ, g and ϱ relate through

$$\varrho(\varphi) = \frac{1}{\gamma(\cos\varphi,\sin\varphi)} = \frac{1}{|\sin\varphi|\, g(\cot(-\varphi))} \qquad \text{and} \qquad g(y) = \frac{\sqrt{1+y^2}}{\varrho(\operatorname{arccot}(-y))}. \tag{2.6}$$

We will use these expressions in Section 9.

Recall that the curvature of the graph of (a sufficiently smooth) u is given by $\varkappa(x, u(x)) = u_{xx}(x)(1 + u_x(x)^2)^{-3/2}$.

Unless stated otherwise, a *minimizer* always denotes a *global* minimizer (which does not have to be unique). In general, our results only depend on the difference of the boundary values

$$\omega \equiv \beta - \alpha,$$

where α and β are as in (2.3). The *straight line* always denotes the function

$$\ell : [0, 1] \to \mathbb{R}, \quad x \mapsto \alpha + \omega x \tag{2.7}$$

whose graph joins the points $(0, \alpha)$ and $(1, \beta)$.

Following Dacorogna [10, § 2.3], for any function $f : \mathbb{R} \to \mathbb{R} \cup \{+\infty\}$, $f \not\equiv +\infty$, we denote by f^{**} its *convex and lower semi-continuous envelope*, namely

$$f^{**}(x) = \sup\left\{\tilde{f}(x) \,\middle|\, \tilde{f} \le f, \tilde{f} \text{ convex and lower semi-continuous}\right\}.$$

(This set is not empty; take for instance the bidual function of f as in [10, Def. 2.41], see also [10, Thm. 2.43].) Note that f^{**} is itself convex and lower semi-continuous [10, Thm. 2.26 3]. A convex and finite map $f : \mathbb{R} \to \mathbb{R}$ is even locally Lipschitz continuous [10, Thm. 2.31]. The subdifferential of a convex function $f : \mathbb{R} \to \mathbb{R} \cup \{+\infty\}$, $f \not\equiv +\infty$ is denoted by ∂f [10, Def. 2.46]. Note that if in addition $f : \mathbb{R} \to \mathbb{R}$ then $\partial f(x) \neq \emptyset$ for all $x \in \mathbb{R}$ [10, Cor. 2.51]; moreover $\partial f(x)$ is a convex and compact set [10, Thm. 2.50 (iii)]. If $\partial f(x)$ is a singleton, i. e. $\#\partial f(x) = 1$, then f is differentiable at x [10, Thm. 2.50 (vi)].

Observe that convexity of g in (2.5) is *equivalent* to sequential weak lower semi-continuity of E_0 in $H^{1,p}$, $p \ge 1$, cf. Buttazzo et al. [8, Thm. 3.3, Thm. 3.5] for more details.

The following sets (see Fierro, Goglione, and Paolini [15]) are crucial for the understanding of the evolution in the non-stationary case. For a given anisotropy g as in (2.5) sufficiently smooth we define the *globally* and *locally* unstable set

$$\mathrm{GUS} := \left\{y \in \mathbb{R} \,\middle|\, g(y) > g^{**}(y)\right\} \qquad \supset \qquad \mathrm{LUS} := \left\{y \in \mathbb{R} \,\middle|\, g''(y) < 0\right\}.$$

The (closed) set where g and its convex envelope coincide is the *globally stable* set

$$\mathrm{GS} := \mathbb{R} \setminus \mathrm{GUS} = \{y \in \mathbb{R} \,|\, g^{**}(y) = g(y)\}.$$

Note that $g^{-1}(\min_{\mathbb{R}} g) \subset \mathrm{GS}$.

We say that g is *convex at* ω if $\omega \in \mathrm{GS}$ and refer to this situation as the *convex case*, not to be confused with the case of a convex anisotropy where $g^{**} \equiv g$ on $\mathbb{R}$.

Finally, $C_0^\infty(0, 1)$ denotes the subspace of compactly supported functions in $C^\infty(0, 1)$.

Stationary case

3 Minimizers of the anisotropic functional

In this section we would like to outline some ideas about existence and (possibly) uniqueness of minimizers for E_0 in $\mathscr{C}_{\alpha,\beta}$ (see (2.4)). Most proofs are intentionally

omitted, however we provide a number of examples to clarify and make plausible our statements. Let g be as in (2.5) and $\omega \equiv \alpha - \beta$. From now on a *generalized tangent* h to g^{**} at ω will denote a line h such that $h(\omega) = g^{**}(\omega)$ and $h \le g^{**} (\le g)$.

Since we would like to minimize E_0 and this functional only depends on the derivative of u, we need to identify the set of "optimal" slopes. To do that we proceed as follows. For arbitrary $\omega \in \mathbb{R}$ and $\lambda \in \partial g^{**}(\omega)$ let the line $h_\lambda : \mathbb{R} \to \mathbb{R}$ be given by $x \mapsto g^{**}(\omega) + \lambda(x - \omega)$. In other words, h_λ is a generalized tangent of g^{**} at ω with slope λ. (Obviously $\lambda = g^{**\prime}(\omega)$ if g^{**} is differentiable at ω.) Since $\int_0^1 h_\lambda(u_x) = g^{**}(\omega)$ for $u \in \mathscr{C}_{\alpha,\beta}$, the functionals E_0 and

$$E_0^\lambda : u \mapsto \int_0^1 (g - h_\lambda)(u_x), \qquad u \in \mathscr{C}_{\alpha,\beta},$$

have the same minimizers. The main idea is now to show that for $\lambda \in \partial g^{**}(\omega)$ the set

$$Z_\lambda := (g - h_\lambda)^{-1}(0)$$

is not empty. This allows for $\inf_{\mathscr{C}_{\alpha,\beta}} E_0^\lambda = 0$. We distinguish between the following possible situations.

Single-slope (convex). *Here $\omega \in$ GS and for each $\lambda \in \partial g^{**}(\omega)$ all* further *points in Z_λ* (if they exist) *lie either above or below ω.* For instance this is the case for $\omega \in \mathrm{GS} \setminus \{2\} = \mathbb{R} \setminus (1,3)$ in Figure 1 and $\omega \in \mathrm{GS} = \{0\}$ in Figure 2. In this situation the straight line (2.7) is the unique minimizer.

Multiple-slope (convex). *Here $\omega \in$ GS and there is a $\lambda \in \partial g^{**}(\omega)$ such that there are points in Z_λ both above and below ω.* (This implies $\partial g^{**}(\omega) = \{g^{**\prime}(\omega)\}$.) In this case there are infinitely many minimizers in $\mathscr{C}_{\alpha,\beta}$, the straight line (2.7) being one of them. For instance consider the situation of Figure 1 where $\omega = 2$ and take a piecewise linear curve with slope 1 on $[0, \frac{1}{2})$ and 3 on $(\frac{1}{2}, 1]$. In a similar way one can construct infinitely many other minimizers.

Non-degenerate (non-convex). *Here $\omega \in \mathrm{GUS} \cap \mathrm{conv\,GS}$.* Note that there are points in $Z_{g^{**\prime}(\omega)}$ both above and below ω. For instance take $\omega \in \mathrm{GUS} = (1,2) \cup (2,3)$ in Figure 1. In this case there are infinitely many piecewise-linear minimizers constructed in a similar way to the (convex) multiple-slope case. The straight line is not a minimizer, and more generally there is no minimizer belonging to C^1.

Degenerate (non-convex). *Here $\omega \in \mathrm{GUS} \setminus \mathrm{conv\,GS}$.* Note that all the points in $Z_{g^{**\prime}(\omega)}$ lie either above or below ω. In this case there are no minimizers in $\mathscr{C}_{\alpha,\beta}$. For example let $\omega \in \mathrm{GUS} = \mathbb{R} \setminus \{0\}$ in Figure 2. Here a minimizing sequence is given for instance by

$$u_k(t) := \begin{cases} \min(\alpha + kt, \beta) & \text{if } \beta > \alpha, \\ \max(\alpha - kt, \beta) & \text{if } \beta < \alpha. \end{cases} \tag{3.1}$$

The proof of the existence of a minimizer in the convex case is straightforward.

Proposition 3.1 (Existence of minimizers in the convex case).
If $\omega \in$ GS then the straight line ℓ as in (2.7) is a minimizer of E_0 in $\mathscr{C}_{\alpha,\beta}$.

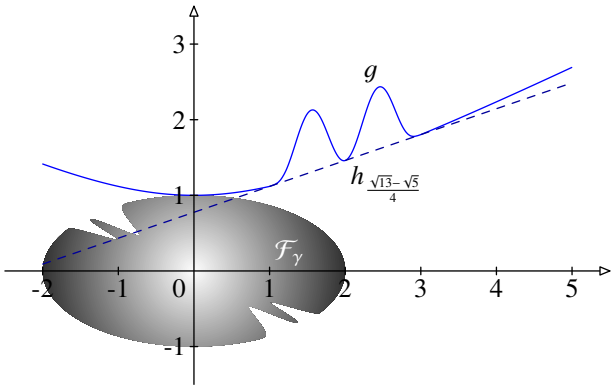

Figure 1: The function g was created by inserting two "bumps" into $y \mapsto \sqrt{1 + \frac{1}{4}y^2}$. The convex envelope g^{**} of g coincides with g on $\mathrm{GS} = \mathbb{R} \setminus ((1,2) \cup (2,3))$ and with $h_{\frac{\sqrt{13}-\sqrt{5}}{4}}$ on $[1,3]$.

Proof. Let $\lambda \in \partial g^{**}(\omega)$. By assumption g^{**} satisfies $g^{**}(y) \geq g^{**}(\omega) + \lambda(y - \omega)$ for all $y \in \mathbb{R}$, see Dacorogna [10, Cor. 2.51]. Thus, for any $u \in \mathscr{C}_{\alpha,\beta}$,

$$E_0(u) = \int_0^1 g(u_x) \geq \int_0^1 g^{**}(u_x) \geq g^{**}(\omega) + \lambda \int_0^1 (u_x - \omega) = g(\omega) = E_0(\ell). \qquad \square$$

We are mainly interested in the non-convex case, in particular in the *non-degenerate* case (since there are no minimizers in the degenerate one). Here it can be shown that g^{**} is linear on some open interval containing ω. As a consequence $g^{**\prime}(\omega)$ exists and Z_λ with $\lambda = g^{**\prime}(\omega)$ contains *at least* one other point above *and* another below ω. We introduce the notation

$$z_\omega^-, z_\omega^+ \in Z_\lambda, \qquad z_\omega^- < \omega < z_\omega^+, \quad \text{and} \quad (z_\omega^-, z_\omega^+) \cap Z_\lambda = \emptyset \tag{3.2}$$

for the smallest point above ω and the largest one below. Although in many situations minimizers can also be constructed using other "slopes" of Z_λ these two points will play a fundamental role in the next section.

4 Regularization as a choice criterion

The aim of this section is to derive a procedure to single out some of the many minimizers existing in the non-degenerate (non-convex) case. (Thus we have in mind a situation like $\omega \in (1,2)$ in Figure 1.) It turns out that the minimizers with the smallest number of discontinuities in the derivative will be selected.

Let $\varepsilon \geq 0$. Obviously,

$$E_\varepsilon : u \mapsto \int_0^1 \left(g(u_x(x)) + \varepsilon^2 \frac{u_{xx}(x)^2}{(1 + u_x(x)^2)^{5/2}} \right) \mathrm{d}x \tag{4.1}$$

contains only first and second derivatives of u. Thus any function $u \in \mathscr{C}_{\alpha,\beta} \cap H^{2,2}(0,1)$

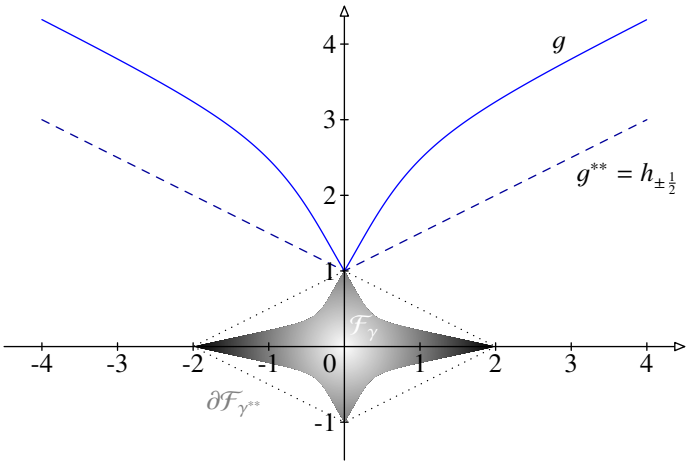

Figure 2: The function ϱ (see (2.6)) is given by $\varphi \mapsto \left(\frac{1}{2} + \sin(2\varphi) + \frac{1}{\pi}\varphi\right)^{-1}$ on $[0, \frac{\pi}{2}]$ and extended by mirroring. We have GUS = LUS = $\mathbb{R} \setminus \{0\}$. One can show $g^{**}(y) = g(0) + g^\infty |y|$ where $g^\infty = \lim_{|y|\to\infty} \frac{g(y)}{|y|} = \frac{1}{2}$.

is a minimizer of E_ε if and only if $v := u_x$ is a minimizer of

$$I_\varepsilon : v \mapsto \int_0^1 \left(g(v(x)) + \varepsilon^2 \frac{v_x(x)^2}{(1 + v(x)^2)^{5/2}} \right) \mathrm{d}x \tag{4.2}$$

in

$$\mathscr{D}_\omega := \left\{ v \in H^{1,2}(0,1) \,\middle|\, \int_0^1 v(x)\,\mathrm{d}x = \omega \right\} = \left\{ u_x \,\middle|\, u \in \mathscr{C}_{\alpha,\beta} \cap H^{2,2}(0,1) \right\}.$$

This section is devoted to the proof of the following

Theorem 4.1 (Minimizers of I_ε). *In the convex case, i. e. $\omega \in \mathrm{GS}$, the constant map $\bar{v} \equiv \omega$ is the unique minimizer of I_ε in $\mathscr{D}_\omega$ for all $\varepsilon \geq 0$.*

In the non-degenerate (non-convex) case, i. e. $\omega \in \mathrm{GUS} \cap \operatorname{conv} \mathrm{GS}$, there exists a minimizer of I_ε in $\mathscr{D}_\omega$ for any $\varepsilon > 0$. Moreover, the following statements hold.

(i) *Each minimizer v_ε takes values in $[z_\omega^-, z_\omega^+]$ only, where $z_\omega^\pm$ is as in (3.2).*

(ii) *For $g \in C^k(\mathbb{R})$, $k = 1, 2, \ldots$, any minimizer belongs to $C^{k+1}([0,1])$ and satisfies the non-linear second order ordinary differential equation*

$$v_{xx} = \frac{(1+v^2)^{5/2}}{2\varepsilon^2}\,(g'(v) + \lambda) + \frac{5v_x^2 v}{2(1+v^2)} \tag{4.7}$$

where

$$\lambda := -\delta I_\varepsilon(v, 1) = \int_0^1 \left(-g'(v) + \frac{5\varepsilon^2 v_x^2 v}{(1+v^2)^{7/2}} \right) \mathrm{d}x \tag{4.4}$$

together with the natural boundary conditions $v_x(0) = v_x(1) = 0$.

(iii) *If v is a minimizer then $v(1-\cdot)$ is also a minimizer. For $g \in C^2(\mathbb{R})$ and $\varepsilon \ll 1$ each minimizer is* strictly *monotone.*

(iv) *Any sequence of monotone increasing I_ε-minimizers converges in L^p, $p \in [1,\infty)$, to*

$$\bar{\bar{v}} := z_\omega^- \chi_{(-\infty,x_*)} + z_\omega^+ \chi_{(x_*,\infty)} \qquad \textit{where} \qquad z_\omega^- x_* + z_\omega^+ (1-x_*) \equiv \omega. \tag{4.11}$$

Here $\chi_\cdot$ denotes the characteristic function.

As a consequence we infer the following important

Corollary 4.2 (Uniform $C^{1,1}$-bound in ε). *Minimizers $v_\varepsilon \in \mathscr{D}_\omega$ for I_ε correspond to E_ε-minimizers*

$$\left(u_\varepsilon : x \mapsto \alpha + \int_0^x v_\varepsilon(\xi)\,\mathrm{d}\xi \right) \in \mathscr{C}_{\alpha,\beta} \cap H^{2,2}(0,1) \tag{4.3}$$

satisfying the uniform bound $\|u_\varepsilon\|_{H^{1,\infty}} \le C$ (independent of ε).

We first consider the convex case $\omega \in \mathrm{GS}$. Obviously, $\bar{v}$ is a minimizer, for $\bar{v} \in \mathscr{D}_\omega$ and $I_\varepsilon(\bar{v}) = I_0(\bar{v}) = \inf_{\mathscr{D}_\omega} I_0 \le \inf_{\mathscr{D}_\omega} I_\varepsilon$, where we have used Proposition 3.1 for the second equality. Uniqueness follows by observing that

$$I_\varepsilon(v) - I_\varepsilon(\bar{v}) = \underbrace{I_\varepsilon(v) - I_0(v)}_{\ge 0} + \underbrace{I_0(v) - \inf_{\mathscr{D}_\omega} I_0}_{\ge 0} \ge 0 \quad \text{for any } v \in \mathscr{D}_\omega,$$

so that any minimizer $v \in \mathscr{D}_\omega$ has to satisfy $0 = I_\varepsilon(v) - I_0(v) = \varepsilon^2 \int_0^1 \frac{v_x^2}{(1+v^2)^{5/2}}$. This gives $v_x \equiv 0$, thus $v \equiv \bar{v}$.

The proof for the non-degenerate (non-convex) case

$$\omega \in \mathrm{GUS} \cap \operatorname{conv} \mathrm{GS} \tag{ND}$$

is split up into several steps which are carried out in the following subsections. As pointed out in the last section for E_0 and E_0^λ, the functionals I_ε and

$$I_\varepsilon^\lambda : v \mapsto \int_0^1 \left((g - h_\lambda)(v) + \varepsilon^2 \frac{v_x^2}{(1+v^2)^{5/2}} \right), \qquad v \in \mathscr{D}_\omega, \quad \lambda \in \partial g^{**}(\omega),$$

have the same minimizers within $\mathscr{D}_\omega$. Note that in the non-convex case we always have $\lambda = g^{**\prime}(\omega)$. For the sake of simplicity, it will sometimes be convenient to consider g to be renormalized to $g - h_{g^{**\prime}(\omega)}$ so that

$$g(z_\omega^\pm) = 0, \qquad g|_{(z_\omega^-, z_\omega^+)} > 0. \tag{R}$$

4.1 Existence

First of all we observe that boundedness of $I_\varepsilon(v)$ does not imply an $H^{1,2}$-bound for v.

Example 4.3 (Boundedness of I_ε does not imply an $H^{1,2}$-bound). Let $\omega \ge 2$ and consider $v_\delta \in C^\infty([0,1])$ defined by $x \mapsto (\delta + x)^{-1/2} + c_\delta$ with $\delta \in (0,1]$ and c_δ chosen so that $\int_0^1 v_\delta = \omega$. Precisely we infer that $c_\delta = \omega - \frac{2}{\sqrt{1+\delta}+\sqrt{\delta}} \ge 0$. We obtain

$v_{\delta,x}(x) = -\frac{1}{2}(\delta + x)^{-3/2}$ so that

$$I_\varepsilon(v_\delta) \le C\,(1 + \|v_\delta\|_{L^1}) + \tfrac{1}{4}\varepsilon^2 \int_0^1 \frac{(\delta + x)^{-1/2}}{\left((\delta + x) + \left(1 + c_\delta \sqrt{\delta + x}\right)^2\right)^{5/2}}\,\mathrm{d}x \le C\,(1 + \omega) + \tfrac{1}{4}\varepsilon^2\omega,$$

where C does not depend on δ. On the other hand,

$$\left\|v_{\delta,x}\right\|_{L^2}^2 = \tfrac{1}{4}\int_0^1 (\delta + x)^{-3}\,\mathrm{d}x \ge \tfrac{1}{8}\left(\delta^{-2} - 1\right) \xrightarrow{\delta \searrow 0} \infty. \qquad \diamond$$

Because of the lack of an estimate for $|v_x|$ we cannot immediately apply direct methods. Instead, we have to employ a refined coercivity argument.

Proposition 4.4 (Minimizers remain in $[z_\omega^-, z_\omega^+]$).
Consider (ND). *Assume* $v \in \mathscr{D}_\omega$ *with* $\operatorname{image} v \not\subset [z_\omega^-, z_\omega^+]$.
Then there exists some $\tilde{v} \in \mathscr{D}_\omega$ *with* $\operatorname{image} \tilde{v} \subset [z_\omega^-, z_\omega^+]$ *and* $I_\varepsilon(\tilde{v}) < I_\varepsilon(v)$.

Proof. Let $\operatorname{image} v \not\subset [z_\omega^-, z_\omega^+]$ and recall $\omega \in (z_\omega^-, z_\omega^+)$. Without loss of generality, we may assume (R). We first consider $[z_\omega^-, z_\omega^+] \subset \operatorname{image} v$. By continuity we may choose $0 \le x_0 < x_1 \le 1$ with $\{v(x_0), v(x_1)\} = \{z_\omega^-, z_\omega^+\}$ and $\operatorname{image} v|_{[x_0,x_1]} = [z_\omega^-, z_\omega^+]$. Define $\hat{v} : \mathbb{R} \to \mathbb{R}$ via

$$\hat{v} : x \longmapsto \begin{cases} v(x_0) & \text{if } x \le x_0, \\ v(x) & \text{if } x \in [x_0, x_1], \\ v(x_1) & \text{if } x \ge x_1. \end{cases}$$

Clearly, $I_\varepsilon(\hat{v}|_{[0,1]}) < I_\varepsilon(v)$ while the volume constraint may be violated. But since we have $I_\varepsilon(\hat{v}(\cdot - \bar{x})|_{[0,1]}) < I_\varepsilon(v)$ for all $\bar{x} \in \mathbb{R}$, by continuity there is some $\hat{x} \in [-x_1, 1 - x_0]$ such that $\tilde{v} := \hat{v}(\cdot - \hat{x})|_{[0,1]} \in \mathscr{D}_\omega$ and $I_\varepsilon(\tilde{v}) < I_\varepsilon(v)$, see Figure 3.

Now we consider $[z_\omega^-, z_\omega^+] \not\subset \operatorname{image} v$. We first assume $\operatorname{image} v \subset (-\infty, z_\omega^+)$; the situation $\operatorname{image} v \subset (z_\omega^-, \infty)$ is symmetric. Since by assumption $\operatorname{image} v \not\subset [z_\omega^-, z_\omega^+]$ we may choose $0 \le \xi_0 < \xi_1 \le 1$ satisfying $v|_{(\xi_0,\xi_1)} < z_\omega^-$ and

$$\left[v(\xi_0) = v(\xi_1) = z_\omega^- \quad \text{or} \quad \left(\text{there is } j \in \{0,1\} \text{ such that } \xi_j = j \text{ and } v(\xi_{1-j}) = z_\omega^-\right)\right].$$

Note that, since $v \in \mathscr{D}_\omega$, some values of v have to be larger than ω (if v only touches ω from below then it has to be equal to ω on the whole interval $[0,1]$). Replacing $v(x)$ by z_ω^- on (ξ_0, ξ_1) leads to a strictly smaller value of I_ε while the volume constraint *is* violated; indeed the volume increased. Now we just enlarge the region where the function is constant equal to z_ω^- until the volume condition is met. More formally, we may choose $\eta_0 \in [0, \xi_0]$, $\eta_1 \in [0, 1 - \xi_1]$ by continuity such that

$$\tilde{v} : x \longmapsto \begin{cases} v(x + \eta_0) & \text{if } x \in [0, \xi_0 - \eta_0], \\ z_\omega^- & \text{if } x \in [\xi_0 - \eta_0, \xi_1 + \eta_1], \\ v(x - \eta_1) & \text{if } x \in [\xi_1 + \eta_1, 1] \end{cases}$$

belongs to $\mathscr{D}_\omega$. By construction, $I_\varepsilon(\tilde{v}) < I_\varepsilon(v)$. We have illustrated the procedure on a single interval. To deal at once with all intervals as above consider the function $\tilde{v} := \max(v, z_\omega^-) \in H^{1,2}$, then "enlarge" one of the intervals where $\tilde{v} \equiv z_\omega^-$ until the volume constraint is satisfied. $\square$

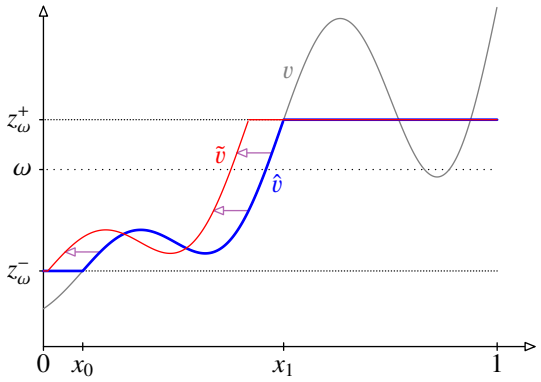

Figure 3: Construction of $\tilde{v}$ in the proof of Proposition 4.4

Lemma 4.5 (Existence of minimizers).
Consider (ND). There exists a minimizer of I_ε in $\mathscr{D}_\omega$ for any $\varepsilon > 0$.

Proof. Let $(v_k)_{k\in\mathbb{N}} \subset \mathscr{D}_\omega$ be a minimizing sequence for I_ε. By Proposition 4.4 we may assume image $v_k \subset [z_\omega^-, z_\omega^+]$ for all $k \in \mathbb{N}$. We obtain

$$\varepsilon^2 \left\|v_{k,x}\right\|_{L^2}^2 \le \varepsilon^2 \left(1 + \max\left|z_\omega^\pm\right|^2\right)^{5/2} \int_0^1 \frac{v_{k,x}^2}{(1+v_k^2)^{5/2}} \le \left(1 + \max\left|z_\omega^\pm\right|^2\right)^{5/2} I_\varepsilon(v_k) \le C < \infty.$$

Passing to a subsequence (always without relabeling), there is some $v_0 \in H^{1,2}$ with $v_k \rightharpoonup v_0$ weakly in $H^{1,2}$ and $v_k \to v_0$ strongly in L^2. By Dacorogna [10, Cor. 3.24], the functional I_ε is sequentially weakly lower semi-continuous. Thus

$$I_\varepsilon(v_0) \le \liminf_{k\to\infty} I_\varepsilon(v_k) = \inf_{\mathscr{D}_\omega} I_\varepsilon.$$

It remains to verify that $v_0 \in \mathscr{D}_\omega$. But this is straightforward since $\left|\int_0^1 v_0 - \omega\right| \le \|v_k - v_0\|_{L^2} \xrightarrow{k\to\infty} 0$. □

4.2 Regularity of local minimizers

Our next task is to derive the Euler-Lagrange equation. We infer regularity not only for minimizers but for all *local* minimizers v of I_ε in $\mathscr{D}_\omega$ (i. e. $v \in \mathscr{D}_\omega$ and there is some $\eta > 0$ with $I_\varepsilon(\tilde{v}) \ge I_\varepsilon(v)$ for all $\tilde{v} \in \mathscr{D}_\omega$ satisfying $\|\tilde{v} - v\|_{H^{1,2}} < \eta$). The results presented in this subsection also apply for the convex cases.

Lemma 4.6 (First variation). *For each $v, w \in H^{1,2}(0,1)$ and $g \in C^1$ the first variation $\delta I_\varepsilon(v,w) := \frac{\mathrm{d}}{\mathrm{d}\tau}\big|_{\tau=0} I_\varepsilon(v+\tau w)$ exists and amounts to*

$$\delta I_\varepsilon(v,w) = \int_0^1 \left(g'(v)w + \frac{2\varepsilon^2 v_x w_x}{(1+v^2)^{5/2}} - \frac{5\varepsilon^2 v_x^2 v w}{(1+v^2)^{7/2}}\right).$$

Proof. We obtain $I_\varepsilon(v+\delta w) - I_\varepsilon(v) = \delta \int_0^1 \int_0^1 \zeta(\delta,\xi,x)\,\mathrm{d}\xi\,\mathrm{d}x$, where

$$\zeta(\delta,\xi,\cdot) := g'(v+\xi\delta w)w + \frac{2\varepsilon^2(v_x+\xi\delta w_x)w_x}{(1+(v+\xi\delta w)^2)^{5/2}} - \frac{5\varepsilon^2(v_x+\xi\delta w_x)^2(v+\xi\delta w)w}{(1+(v+\xi\delta w)^2)^{7/2}}.$$

Using the growth conditions on g and the continuity of g', the integral $\int_0^1 \zeta(\delta,\xi,\cdot)\,\mathrm{d}\xi$ is majorized by some L^1 function uniformly in δ on some neighbourhood of 0. Applying Lebesgue's theorem on dominated convergence, we may pass to the limit. □

Note that we do not obtain the above result for $g \in C^{0,1}$ as $g' \circ v$ might be undefined on a positive measure set.

Defining

$$\lambda := -\delta I_\varepsilon(v,1) = \int_0^1 \left(-g'(v) + \frac{5\varepsilon^2 v_x^2 v}{(1+v^2)^{7/2}}\right)\mathrm{d}x \tag{4.4}$$

and noting that for each $\delta \in \mathbb{R}$, $\varphi \in H^{1,2}$, and $w := \varphi - \int_0^1 \varphi \in H^{1,2}(0,1)$ we obtain $v + \delta w \in \mathscr{D}_\omega$, we infer

Lemma 4.7 (Weak Euler-Lagrange equation). *Let v be a local minimizer of I_ε in $\mathscr{D}_\omega$ and $g \in C^1$. Then there is some $\lambda \in \mathbb{R}$ with*

$$\delta I_\varepsilon(v,\varphi) + \lambda \int_0^1 \varphi = 0 \qquad \text{for all } \varphi \in H^{1,2}(0,1).$$

For $\varphi \in H_0^{1,2}(0,1)$, the weak Euler-Lagrange equation reads

$$\begin{aligned} 0 &= \int_0^1 \left(g'(v)\varphi + \frac{2\varepsilon^2 v_x\varphi_x}{(1+v^2)^{5/2}} - \frac{5\varepsilon^2 v_x^2 v\varphi}{(1+v^2)^{7/2}} + \lambda\varphi\right) \\ &= \int_0^1 \varphi_x \left(\frac{2\varepsilon^2 v_x}{(1+v^2)^{5/2}} - \lambda x + \int_0^x \frac{5\varepsilon^2 v_x^2 v}{(1+v^2)^{7/2}} - \int_0^x g'(v)\right). \end{aligned} \tag{4.5}$$

Since the bracket belongs to L^1 we may apply DuBois-Reymond's Lemma, cf. Buttazzo et al. [8, Lem. 1.8], which gives

$$v_x = \frac{(1+v^2)^{5/2}}{2\varepsilon^2}\left(\lambda x + c + \int_0^x g'(v) - \int_0^x \frac{5\varepsilon^2 v_x^2 v}{(1+v^2)^{7/2}}\right) \tag{4.6}$$

for some constant $c \in \mathbb{R}$. Assuming $g \in C^1$ we obtain $g'(v) \in C^0$ so that $\int g'(v) \in C^1$. Moreover, since $v_x^2 \in L^1$ the right-hand side of (4.6) belongs to $H^{1,1} \hookrightarrow L^4$ [8, Thm. 2.8]. This gives $v_x \in L^4$ and therefore $5\varepsilon^2 v_x^2 v(1+v^2)^{-7/2} \in L^2$. Thus, the right-hand side of (4.6) belongs to $H^{1,2}$ which implies $v \in H^{2,2}$. From $H^{2,2}(0,1) \subset C^1([0,1])$ and (4.6) it follows that $v \in C^2$ which cannot be improved without imposing stronger conditions on g.

Integrating by parts in (4.5) and applying the Fundamental Lemma we deduce

$$v_{xx} = \frac{(1+v^2)^{5/2}}{2\varepsilon^2}(g'(v)+\lambda) + \frac{5v_x^2 v}{2(1+v^2)}. \tag{4.7}$$

By a bootstrap argument we infer higher regularity for $k = 1, 2, \ldots$.

Thus we have proven

Lemma 4.8 (Regularity of local minimizers). *For $\varepsilon > 0$ and $g \in C^k(\mathbb{R})$, $k = 1, 2, \dots$, a local minimizer of I_ε in $\mathscr{D}_\omega$ belongs to $C^{k+1}([0,1])$ and satisfies (4.7).*

We may obtain similar results if g belongs to suitable Hölder or Sobolev spaces.

Integrating by parts in (4.5) for arbitrary $\varphi \in H^{1,2}(0,1)$ yields

Corollary 4.9 (Natural boundary conditions). *For $\varepsilon > 0$ and $g \in C^1(\mathbb{R})$, a local minimizer of I_ε in $\mathscr{D}_\omega$ satisfies $v_x(0) = v_x(1) = 0$.*

Finally, multiplying (4.7) by v_x and integrating, we obtain

$$\varepsilon^2 \frac{v_x^2}{(1+v^2)^{5/2}} = g(v) + \lambda v + \sigma \tag{4.8}$$

for some integration constant $\sigma \in \mathbb{R}$. Note that (4.7) and (4.8) are autonomous nonlinear second- / first-order ordinary differential equations.

4.3 Monotonicity of local minimizers

As in the preceding subsection we consider not only global minimizers but also local ones while we again restrict to the non-degenerate (non-convex) case. Note that *a priori* we cannot exclude that a local minimizer is constant, since these satisfy the Euler-Lagrange Equation (4.7). (See also Corollary 4.13 below.)

A main property in the study of autonomous systems is that orbits cannot intersect each other. Employing an argument as in Carr, Gurtin, and Slemrod [9] we derive

Proposition 4.10 (Local minimizers are monotone). *Consider* (ND).
If $g \in C^2$, any local *minimizer for I_ε in $\mathscr{D}_\omega$ is either constant or* strictly *monotone.*

The reason for the restriction to $g \in C^2$ is again that we have to ensure that $g'' \circ v$ is well-defined.

Proof. We may assume (R) (see page 10) without loss of generality. Let v be a non-constant local minimizer of I_ε in $\mathscr{D}_\omega$. Thus the Lagrange multiplier λ can be considered a fixed constant (which can be computed according to (4.4)). We may rewrite the Euler-Lagrange Equation (4.7) as an autonomous system of two first-order ordinary differential equations $\binom{\xi}{\eta}_x = F(\xi,\eta) = \binom{F_1(\xi,\eta)}{F_2(\xi,\eta)}$, where $F_1(\xi,\eta) = \eta$, $F_2(\xi,\eta) = \frac{1}{2\varepsilon^2}(1+\xi^2)^{5/2}(g'(\xi)+\lambda) + \frac{5}{2}\xi(1+\xi^2)^{-1}\eta^2$. Of course, $(\xi,\eta) = (v, v_x)$ is a solution.

We divide our proof into two steps.

(i) The solution (v, v_x) lies on a *closed* orbit. This orbit is symmetric with respect to the ξ-axis and intersects it precisely twice.

(ii) The (image of the) solution (v, v_x) does not entirely cover the orbit.

Recalling the natural boundary conditions $v_x(0) = v_x(1) = 0$ due to Corollary 4.9, the solution (v, v_x) starts and ends at the ξ-axis. As $v_x \not\equiv 0$, we obtain by means of (i) and (ii) either $v_x > 0$ or $v_x < 0$ on $(0,1)$.

(i) Obviously $F(\xi,-\eta)=\binom{-F_1(\xi,\eta)}{F_2(\xi,\eta)}$, so the phasefield is "symmetric" with respect to the ξ-axis which gives symmetry of the orbits. We already know $v\in C^3$ from Lemma 4.8, so (as v is not constant) there is a $\theta\in(0,1]$ such that v_x is either positive or negative on $(0,\theta)$ and $v_x(\theta)=0$. Now by symmetry, $\binom{v}{-v_x}(\theta-\cdot)$ is also a solution for our system belonging to the same orbit. By the Picard-Lindelöf Theorem this defines the unique extension to our solution. Thus we have shown that the orbit corresponding to (v,v_x) is closed.

(ii) Assuming the contrary, (v,v_x) covers the orbit. So there is some $x_0\in(0,1]$ such that $v(0)=v(x_0)$. From (i) we infer $v_x(0)=v_x(x_0)=0$. Our aim is to show that there is some $\phi\in H^{1,2}$ with $\int_0^1\phi=0$ (so that $v+\tau\phi\in\mathscr{D}_\omega$ for all $\tau\in\mathbb{R}$) and $\delta^2 I_\varepsilon(v;\phi,\phi)<0$, where $\delta^2 I_\varepsilon$ denotes the second variation of I_ε.

Argueing as in the proof of Lemma 4.6 we obtain the existence of the second variation

$$\begin{aligned}
&\delta^2 I_\varepsilon(v;\phi,\phi):=\left.\tfrac{\mathrm{d}^2}{\mathrm{d}\tau^2}\right|_{\tau=0} I_\varepsilon(v+\tau\phi)\\
&=\varepsilon^2\int_0^1\left(\frac{g''(v)}{\varepsilon^2}\phi^2+2\frac{\phi_x^2}{(1+v^2)^{5/2}}-20\frac{vv_x\phi\phi_x}{(1+v^2)^{7/2}}-5\frac{v_x^2\phi^2}{(1+v^2)^{7/2}}+35\frac{v_x^2v^2\phi^2}{(1+v^2)^{9/2}}\right).
\end{aligned}$$

Recalling Lemma 4.8 we define $\phi_0\in H^{1,2}(0,1)$ by $\phi_0:=v_x$ on $[0,x_0]$ and $\phi_0:=0$ on $[x_0,1]$. Furthermore we choose $\phi_1\in H^{1,2}(0,1)$ satisfying $\phi_1(0)=1$, $\phi_1\equiv 0$ on $[x_0,1]$, and $\int_0^1\phi_1=0$. So $\phi:=\phi_0+\theta\phi_1$ fulfills $\int_0^1\phi=0$ for all $\theta\in\mathbb{R}$. It remains to show that we can achieve $\delta^2 I_\varepsilon(v;\phi,\phi)<0$ by choosing θ properly. Now

$$\begin{aligned}
&\frac{\delta^2 I_\varepsilon(v;\phi,\phi)}{\varepsilon^2}\\
&=\int_0^{x_0}\left(\frac{g''(v)}{\varepsilon^2}v_x^2+2\frac{v_{xx}^2}{(1+v^2)^{5/2}}-20\frac{v_{xx}v_x^2v}{(1+v^2)^{7/2}}-5\frac{v_x^4}{(1+v^2)^{7/2}}+35\frac{v_x^4v^2}{(1+v^2)^{9/2}}\right)\\
&\quad+2\theta\int_0^{x_0}\left(\frac{g''(v)}{\varepsilon^2}v_x\phi_1+2\frac{v_{xx}\phi_{1,x}}{(1+v^2)^{5/2}}-10\frac{v_x^2v\phi_{1,x}+v_{xx}v_xv\phi_1}{(1+v^2)^{7/2}}-5\frac{v_x^3\phi_1}{(1+v^2)^{7/2}}\right.\\
&\qquad\left.+35\frac{v_x^3v^2\phi_1}{(1+v^2)^{9/2}}\right)\\
&\quad+\theta^2\int_0^{x_0}\left(\frac{g''(v)}{\varepsilon^2}\phi_1^2+2\frac{\phi_{1,x}^2}{(1+v^2)^{5/2}}-20\frac{vv_x\phi_1\phi_{1,x}}{(1+v^2)^{7/2}}-5\frac{v_x^2\phi_1^2}{(1+v^2)^{7/2}}+35\frac{v_x^2v^2\phi_1^2}{(1+v^2)^{9/2}}\right)\\
&=:\mathrm{I}+\theta\,\mathrm{II}+\theta^2\mathrm{III}.
\end{aligned}\tag{4.9}$$

The proof is completed by showing that this expression is equal to $-4\theta\frac{v_{xx}(0)}{(1+v(0)^2)^{5/2}}+O(\theta^2)$ and that $v_{xx}(0)\neq 0$. In this case we can find some $\theta\in\mathbb{R}$ with the desired property.

Multiplying (4.7) by $2(1+v^2)^{-5/2}$ and differentiating with respect to x we obtain

$$2\frac{v_{xxx}}{(1+v^2)^{5/2}}=\frac{g''(v)}{\varepsilon^2}v_x+20\frac{v_{xx}v_xv}{(1+v^2)^{7/2}}+5\frac{v_x^3}{(1+v^2)^{7/2}}-35\frac{v_x^3v^2}{(1+v^2)^{9/2}}.\tag{4.10}$$

Multiplying this identity by v_x and substituting it in the first term in (4.9) yields

$$\begin{aligned}
\mathrm{I}&=2\int_0^{x_0}\left(\frac{v_{xx}^2}{(1+v^2)^{5/2}}+\frac{v_{xxx}v_x}{(1+v^2)^{5/2}}-20\frac{v_{xx}v_x^2v}{(1+v^2)^{7/2}}-5\frac{v_x^4}{(1+v^2)^{7/2}}+35\frac{v_x^4v^2}{(1+v^2)^{9/2}}\right)\\
&=2\left[\frac{v_{xx}v_x}{(1+v^2)^{5/2}}-5\frac{v_x^3v}{(1+v^2)^{7/2}}\right]_0^{x_0}=0
\end{aligned}$$

by the natural boundary conditions. We proceed to the second term in (4.9) which by inserting (4.10) multiplied by ϕ_1 becomes

$$\begin{aligned}\mathrm{II} &= 4\int_0^{x_0}\left(\frac{v_{xxx}\phi_1}{(1+v^2)^{5/2}}+\frac{v_{xx}\phi_{1,x}}{(1+v^2)^{5/2}}-10\frac{v_{xx}v_xv\phi_1}{(1+v^2)^{7/2}}-5\frac{v_x^2v\phi_{1,x}+v_{xx}v_xv\phi_1}{(1+v^2)^{7/2}}\right.\\ &\qquad\left.-5\frac{v_x^3\phi_1}{(1+v^2)^{7/2}}+35\frac{v_x^3v^2\phi_1}{(1+v^2)^{9/2}}\right)\\ &= 4\left[\frac{v_{xx}\phi_1}{(1+v^2)^{5/2}}-5\frac{v_x^2v\phi_1}{(1+v^2)^{7/2}}\right]_0^{x_0}=-4\frac{v_{xx}(0)}{(1+v(0)^2)^{5/2}}.\end{aligned}$$

The third term III is easily shown to be $O(1)$. Finally we only have to show $v_{xx}(0)\neq 0$. Indeed if $v_{xx}(0)=0$, by $v_x(0)=0$, the initial velocity of the phase field at the point $(\xi,\eta)=(v(0),v_x(0))$ is $(v_x(0),v_{xx}(0))=(0,0)$, i. e. we are looking at a constant solution. □

From now on we again restrict to (global) minimizers.

Remark 4.11 (Uniqueness of minimizers). Under certain conditions on the regularity of g we expect the uniqueness result by Carr, Gurtin, and Slemrod [9] to carry over to our situation. So, for any $0<\varepsilon\ll 1$, there should be precisely two minimizers $v_{\varepsilon,\nearrow}$, $v_{\varepsilon,\searrow}$ in $\mathscr{D}_\omega$, where $v_{\varepsilon,\nearrow}$ is monotone increasing and $v_{\varepsilon,\searrow}=v_{\varepsilon,\nearrow}(1-\cdot)$ is monotone decreasing. ◇

4.4 Convergence

In this subsections we prove convergence to the limit function

$$\bar{\bar{v}}:=z_\omega^-\chi_{(-\infty,x_*)}+z_\omega^+\chi_{(x_*,\infty)}\qquad\text{where}\qquad z_\omega^-x_*+z_\omega^+(1-x_*)\equiv\omega. \tag{4.11}$$

As before, $\chi_\cdot$ denotes the characteristic function.

Similarly to the convex case where $I_\varepsilon^\lambda(\bar{v})=0$ for any $\varepsilon\geq 0$ and $\lambda\in\partial g^{**}(\omega)$ we establish

Lemma 4.12 (Lower bound for I_ε). *Consider* (ND). *For $\lambda=g^{**\prime}(\omega)$ we obtain*

$$\inf_{\mathscr{D}_\omega} I_\varepsilon^\lambda=O(\varepsilon). \tag{4.12}$$

Proof. Assuming (R) for simplicity, the result follows by showing $I_\varepsilon(w_\varepsilon)=O(\varepsilon)$ for a suitable sequence $(w_\varepsilon)_{\varepsilon>0}\subset\mathscr{D}_\omega$. Let $x_*\in(0,1)$ be as in (4.11) and define a piecewise linear $w_\delta\in\mathscr{D}_\omega$, $0<\delta\ll 1$, via

$$w_\delta : x\longmapsto\begin{cases} z_\omega^- & \text{if } x\in[0,x_*-\delta],\\ \frac{z_\omega^++z_\omega^-}{2}+\frac{z_\omega^+-z_\omega^-}{2\delta}(x-x_*) & \text{if } x\in[x_*-\delta,x_*+\delta],\\ z_\omega^+ & \text{if } x\in[x_*+\delta,1].\end{cases}$$

Now

$$0\leq\inf_{\mathscr{D}_\omega} I_\varepsilon\leq\int_{x_*-\delta}^{x_*+\delta} g(w_\delta)+\varepsilon^2\int_{x_*-\delta}^{x_*+\delta}\frac{w_{\delta,x}^2}{(1+w_\delta^2)^{5/2}}\leq 2\delta\max_{[z_\omega^-,z_\omega^+]} g+\varepsilon^2\frac{(z_\omega^+-z_\omega^-)^2}{2\delta}.$$

Choosing $\delta:=\varepsilon$ yields the desired result. □

As a consequence of the preceding Lemma and Proposition 4.10 we deduce

Corollary 4.13 (No straight line minimizer). *Consider* (ND). *The constant* $\bar{v} \equiv \omega$ *is not a minimizer of* I_ε *in* $\mathscr{D}_\omega$ *for* $0 < \varepsilon \ll 1$. *Moreover, if* $g \in C^2$, *each minimizer of* I_ε *in* $\mathscr{D}_\omega$ *is strictly monotone provided* $0 < \varepsilon \ll 1$.

Proposition 4.14 (Convergence of minimizers). *Consider* (ND). *Let* $(v_\varepsilon)_{\varepsilon>0} \subset \mathscr{D}_\omega$ *be a sequence of monotone increasing minimizers for* I_ε. *Then* $v_\varepsilon \to \bar{\bar{v}}$ *in* L^p, $p \in [1,\infty)$, *as* $\varepsilon \searrow 0$, *where* $\bar{\bar{v}}$ *is as in* (4.11).

Proof. We assume (R). Proposition 4.4 yields image $v_\varepsilon \subset [z_\omega^-, z_\omega^+]$. Let $\mu := \min\left|\omega - z_\omega^\pm\right|$. For $\varepsilon > 0$ and $\eta \in (0,\mu)$ to be chosen later on we define

$$B_{\varepsilon,\eta} := \left\{x \in [0,1] \,\middle|\, \operatorname{dist}(v_\varepsilon(x), z_\omega^-) \geq \eta \text{ and } \operatorname{dist}(v_\varepsilon(x), z_\omega^+) \geq \eta\right\}.$$

We obtain

$$\left|B_{\varepsilon,\eta}\right| \min_{[z_\omega^- + \eta, z_\omega^+ - \eta]} g \leq \int_{B_{\varepsilon,\eta}} g(v_\varepsilon) \leq I_\varepsilon(v_\varepsilon),$$

which gives by Lemma 4.12

$$\left|B_{\varepsilon,\eta}\right| \xrightarrow{\varepsilon \searrow 0} 0 \qquad \text{pointwise for any } \eta \in (0,\mu). \tag{4.13}$$

We will show below the existence of $\varepsilon_1 = \varepsilon_1(\eta) > 0$ with

$$\left\{x \in [0,1] \,\middle|\, \operatorname{dist}(v_\varepsilon(x), z_\omega^-) < \eta\right\} \neq \emptyset \quad \text{and} \quad \left\{x \in [0,1] \,\middle|\, \operatorname{dist}(v_\varepsilon(x), z_\omega^+) < \eta\right\} \neq \emptyset \tag{4.14}$$

for any $\varepsilon \in (0,\varepsilon_1)$. By (4.14) we can define

$$\begin{aligned} b_{\varepsilon,\eta}^- &:= \sup\left\{x \in [0,1] \,\middle|\, \operatorname{dist}(v_\varepsilon(x), z_\omega^-) < \eta\right\} = \sup\left\{x \in [0,1] \,\middle|\, v_\varepsilon(x) < z_\omega^- + \eta\right\}, \\ b_{\varepsilon,\eta}^+ &:= \inf\left\{x \in [0,1] \,\middle|\, \operatorname{dist}(v_\varepsilon(x), z_\omega^+) < \eta\right\} = \inf\left\{x \in [0,1] \,\middle|\, v_\varepsilon(x) > z_\omega^+ - \eta\right\} \end{aligned}$$

in $[0,1]$ for any $\varepsilon \in (0,\varepsilon_1)$. Note that $z_\omega^- + \eta < \omega < z_\omega^+ - \eta$. By monotonicity we infer $B_{\varepsilon,\eta} = \left[b_{\varepsilon,\eta}^-, b_{\varepsilon,\eta}^+\right]$. Making ε_1 smaller if necessary, we will show

$$\max\left|b_{\varepsilon,\eta}^\pm - x_*\right| \leq \frac{\eta}{z_\omega^+ - z_\omega^-} \tag{4.15}$$

for any $\varepsilon \in (0,\varepsilon_1)$. Let $\delta > 0$ and choose

$$\eta = \eta(\delta) := \min\left(\left(\tfrac{1}{2}\delta\right)^{1/p}, \tfrac{1}{4}\delta\left(z_\omega^+ - z_\omega^-\right)^{1-p}, \tfrac{1}{2}\mu\right).$$

It follows by (4.15)

$$\begin{aligned} \left\|v_\varepsilon - \bar{\bar{v}}\right\|_{L^p}^p &\leq \int_0^{\min\left(b_{\varepsilon,\eta}^-, x_*\right)} \left|v_\varepsilon - \bar{\bar{v}}\right|^p + \int_{\min\left(b_{\varepsilon,\eta}^-, x_*\right)}^{\max\left(b_{\varepsilon,\eta}^+, x_*\right)} \left|v_\varepsilon - \bar{\bar{v}}\right|^p + \int_{\max\left(b_{\varepsilon,\eta}^+, x_*\right)}^1 \left|v_\varepsilon - \bar{\bar{v}}\right|^p \\ &\leq \eta^p + \left(z_\omega^+ - z_\omega^-\right)^p \left(\max\left(b_{\varepsilon,\eta}^+, x_*\right) - \min\left(b_{\varepsilon,\eta}^-, x_*\right)\right) \\ &\leq \eta^p + 2\eta\left(z_\omega^+ - z_\omega^-\right)^{p-1} \leq \delta \end{aligned}$$

for any $\varepsilon \in (0, \varepsilon_1(\eta(\delta)))$ as desired.

We still have to verify (4.14) and (4.15). For the former we assume

$$\left\{x \in [0,1] \,\middle|\, \operatorname{dist}(v_{\varepsilon_j}(x), z_\omega^-) < \eta\right\} = \emptyset$$

for a sequence $\varepsilon_j \searrow 0$. This means $\operatorname{dist}(v_{\varepsilon_j}(x), z_\omega^-) \geq \eta$ for all $x \in [0,1]$ which implies $\operatorname{dist}(v_{\varepsilon_j}(\cdot), z_\omega^+) < \eta$ on $[0,1] \setminus B_{\varepsilon_j,\eta}$. Since image $v_{\varepsilon_j} \in [z_\omega^-, z_\omega^+]$ and (4.13) we obtain

$$\left|\omega - z_\omega^+\right| = \left|\int_0^1 v_{\varepsilon_j} - z_\omega^+\right| \leq \eta\left(1 - \left|B_{\varepsilon_j,\eta}\right|\right) + (z_\omega^+ - z_\omega^-)\left|B_{\varepsilon_j,\eta}\right| \xrightarrow{j\to\infty} \eta$$

which is a contradiction since we assumed $\eta < \mu \leq \left|\omega - z_\omega^+\right|$. The argument for $b_{\varepsilon,\eta}^+$ is analogous.

To derive (4.15), we again argue by contradiction. Assume that there is a sequence $\varepsilon_j \searrow 0$ with $\left|b_{\varepsilon_j,\eta}^- - x_*\right| > \dfrac{\eta}{z_\omega^+ - z_\omega^-}$. By compactness we may assume $b_{\varepsilon_j,\eta}^- \to \hat{x}_*$ as $j \to \infty$ for some limit point $x_* \in [0,1]$. Using (4.13) we derive

$$\max\left(b_{\varepsilon_j,\eta}^+, \hat{x}_*\right) - \min\left(b_{\varepsilon_j,\eta}^-, \hat{x}_*\right) \leq \left|b_{\varepsilon_j,\eta}^+ - \hat{x}_*\right| + \left|b_{\varepsilon_j,\eta}^- - \hat{x}_*\right| \leq \left|B_{\varepsilon_j,\eta}\right| + 2\left|b_{\varepsilon_j,\eta}^- - \hat{x}_*\right| \xrightarrow{j\to\infty} 0.$$

For $\hat{\omega} := z_\omega^- \hat{x}_* + z_\omega^+(1 - \hat{x}_*)$ we obtain

$$\begin{aligned}
|\omega - \hat{\omega}| = \left|\int_0^1 v_{\varepsilon_j} - \hat{\omega}\right| &\leq \int_0^{\min\left(b_{\varepsilon_j,\eta}^-, \hat{x}_*\right)} \left(v_{\varepsilon_j} - z_\omega^-\right) + \int_{\max\left(b_{\varepsilon_j,\eta}^+, \hat{x}_*\right)}^1 \left(z_\omega^+ - v_{\varepsilon_j}\right) \\
&\quad + \int_{\min\left(b_{\varepsilon_j,\eta}^-, \hat{x}_*\right)}^{\max\left(b_{\varepsilon_j,\eta}^+, \hat{x}_*\right)} \left(\left|v_{\varepsilon_j}\right| + \left|z_\omega^-\right| + \left|z_\omega^+\right|\right) \\
&\leq \eta + 2\left(\left|z_\omega^-\right| + \left|z_\omega^+\right|\right)\left(\max\left(b_{\varepsilon_j,\eta}^+, \hat{x}_*\right) - \min\left(b_{\varepsilon_j,\eta}^-, \hat{x}_*\right)\right).
\end{aligned}$$

Letting $j \to \infty$ we deduce $|\omega - \hat{\omega}| \leq \eta$. From $x_* = \dfrac{z_\omega^+ - \omega}{z_\omega^+ - z_\omega^-}$ and $\hat{x}_* = \dfrac{z_\omega^+ - \hat{\omega}}{z_\omega^+ - z_\omega^-}$ we infer

$$|\hat{x}_* - x_*| \leq \frac{|\hat{\omega} - \omega|}{z_\omega^+ - z_\omega^-} \leq \frac{\eta}{z_\omega^+ - z_\omega^-} \quad \text{which implies} \quad \left|b_{\varepsilon_j,\eta}^- - x_*\right| \leq \left|b_{\varepsilon_j,\eta}^- - \hat{x}_*\right| + \frac{\eta}{z_\omega^+ - z_\omega^-}.$$

Passing to the limit yields a contradiction to our initial assumption $\left|b_{\varepsilon_j,\eta}^- - x_*\right| > \dfrac{\eta}{z_\omega^+ - z_\omega^-}$. The same reasoning applies to $b_{\varepsilon_j,\eta}^+$. □

We close this section with some comments.

Remark 4.15 (Estimate (4.12) cannot be improved). For any sequence $(v_\varepsilon)_{\varepsilon>0} \subset \mathscr{D}_\omega$ of monotone increasing (continuous) minimizers, the preceding lemma gives $v_\varepsilon(0) \to z_\omega^-$ and $v_\varepsilon(1) \to z_\omega^+$ as $\varepsilon \searrow 0$ so that

$$\liminf_{\varepsilon\searrow 0} \inf_{\mathscr{D}_\omega} \frac{I_\varepsilon}{\varepsilon} \geq 2\int_{z_\omega^-}^{z_\omega^+} \frac{\sqrt{g(s)}}{(1+s^2)^{5/4}}\,\mathrm{d}s \overset{(\mathrm{R})}{>} 0.$$

The functional on the right-hand side is the candidate for the Gamma-limit, see Braides [6, Chap. 6]. ◇

Remark 4.16 (Non-existence of minimizers for $\varepsilon = 0$). Assume (R). By Lemma 4.12, a minimizer v_0 of I_0 in $\mathscr{D}_\omega$ has to satisfy $g(v_0) = 0$ a. e. so that $v_0 \in \{z_\omega^\pm\}$ a. e. In order to fulfill the volume constraint, v_0 has to be discontinuous and therefore cannot belong to $\mathscr{D}_\omega \subset C^0$. At least, $v_0 \in L^\infty$. ◇

Remark 4.17 (Unique minimizer for $\varepsilon = \infty$). For fixed $\varepsilon > 0$ the functionals $\varepsilon^\mu I_\varepsilon$, $\mu \in \mathbb{R}$, have the same minimizer. Obviously, $\varepsilon^{-2} I_\varepsilon$ tends (pointwise) to the Willmore functional $I_1 - I_0$ as $\varepsilon \nearrow \infty$. Its unique minimizer in $\mathscr{D}_\omega$ amounts to $\bar{v}$. ◇

Remark 4.18 (Gamma-convergence). In Proposition 4.14 we have established the convergence of a sequence $(v_\varepsilon)_{\varepsilon>0}$ of I_ε-minimizers to the limit function $\bar{\bar{v}}$. Although I_0 does not have minimizers in $\mathscr{D}_\omega$ by Remark 4.16, the map $\bar{\bar{v}}$ is clearly one of many minimizers of I_0 when considered in the class

$$\left\{ v \in L^1(0,1) \,\middle|\, \int_0^1 v(x)\,\mathrm{d}x = \omega \right\}.$$

Observe how the regularization process selects those minimizers with the smallest number of discontinuities.

We could have obtained this piece of information by employing Gamma-convergence arguments, see Braides [6, Chap. 6]. More precisely, under suitable conditions the rescaled energies $\frac{1}{\varepsilon} I_\varepsilon$ Gamma-converge to a functional $\tilde{I}$ that is defined on piecewise constant functions taking values $z_\omega^\pm$ a. e. and that essentially counts the number of jumps. ◇

Evolution equation

For the remainder of this work we assume that g as in (2.5) is at least C^2.

5 Classical formulation of the flow

To derive a classical formulation for the flow we need to compute the first variation for E_ε (cf. (1.2) and (4.1)). Moreover since we consider a fourth-order problem we also need to impose an additional set of boundary conditions: a natural choice is given by the natural boundary conditions. To derive them, assume that $u \in \mathscr{C}_{\alpha,\beta}$ is a smooth critical point for E_ε and consider variations of type $u + \delta\varphi$, where $\varphi \in C^\infty([0,1])$ and $\varphi(0) = \varphi(1) = 0$. We obtain

$$\begin{aligned} 0 = \frac{d}{d\delta}\Big|_{\delta=0} E_\varepsilon(u+\delta\varphi) &= \int_0^1 g'(u_x)\varphi_x + \varepsilon^2 \left(2\frac{u_{xx}\varphi_{xx}}{(1+(u_x)^2)^{5/2}} - 5\frac{(u_{xx})^2 u_x \varphi_x}{(1+(u_x)^2)^{7/2}} \right) dx \\ &= \int_0^1 -(g'(u_x))_x \varphi + 5\varepsilon^2 \left(\frac{(u_{xx})^2 u_x}{(1+(u_x)^2)^{7/2}} \right)_x \varphi - 2\varepsilon^2 \left(\frac{u_{xx}}{(1+(u_x)^2)^{5/2}} \right)_x \varphi_x \, dx \\ &\quad + 2\varepsilon^2 \Big[\frac{u_{xx}\varphi_x}{(1+(u_x)^2)^{5/2}} \Big]_0^1 \qquad \forall \varphi \in C^\infty([0,1]), \varphi(0) = \varphi(1) = 0. \end{aligned}$$

If we choose $\varphi \in C_0^\infty(0,1)$ then we infer that the above integral expression vanishes, therefore we get that

$$0 = \Big[\frac{u_{xx}\varphi_x}{(1+(u_x)^2)^{5/2}} \Big]_0^1 \qquad \forall \varphi \in C^\infty([0,1]), \varphi(0) = \varphi(1) = 0.$$

This implies that the natural boundary conditions are given by

$$u_{xx}(0) = u_{xx}(1) = 0. \tag{5.1}$$

To compute the first variation assume again that $u \in \mathscr{C}_{\alpha,\beta}$ is as smooth as required and let $\varphi \in C_0^\infty(0,1)$. Then

$$\begin{aligned}
&\frac{d}{d\delta}\Big|_{\delta=0} E_\varepsilon(u+\delta\varphi) = \int_0^1 -(g'(u_x))_x\varphi + 5\varepsilon^2\left(\frac{(u_{xx})^2u_x}{(1+(u_x)^2)^{7/2}}\right)_x\varphi + 2\varepsilon^2\left(\frac{u_{xx}}{(1+(u_x)^2)^{5/2}}\right)_{xx}\varphi\,dx \\
&= \int_0^1 \left(-(g'(u_x))_x + \varepsilon^2\left(2\frac{u_{xxxx}}{(1+(u_x)^2)^{5/2}} - 20\frac{u_xu_{xx}u_{xxx}}{(1+(u_x)^2)^{7/2}} + \frac{(u_{xx})^3}{(1+(u_x)^2)^{9/2}}(30(u_x)^2-5)\right)\right)\varphi\,dx \\
&\Big(= \int_0^1 \left(-g''(u_x)u_{xx} + \varepsilon^2(2\varkappa_{ss}+\varkappa^3)\right)\langle -\nu, \begin{pmatrix} 0 \\ \varphi \end{pmatrix}\rangle_{\mathbb{R}^2}\sqrt{1+u_x^2}\,dx\Big),
\end{aligned}$$

where $\frac{d}{ds} = \frac{1}{\sqrt{1+u_x^2}}\frac{d}{dx}$. Using the above piece of information and the expression of the velocity in the graph case we infer that a classical formulation for the flow of E_ε amounts to finding u such that

$$\frac{u_t}{\sqrt{1+u_x^2}} = g''(u_x)u_{xx} - \frac{\varepsilon^2}{(1+u_x^2)^{1/2}}\left(2\frac{u_{xxxx}}{(1+u_x^2)^2} - 20\frac{u_xu_{xx}u_{xxx}}{(1+u_x^2)^3} + \frac{u_{xx}^3}{(1+u_x^2)^4}(30u_x^2-5)\right) \tag{5.2}$$

and subject to the boundary conditions

$$u(0) = \alpha, \quad u(1) = \beta, \quad u_{xx}(0) = u_{xx}(1) = 0. \tag{5.3}$$

Remark 5.1. Note that with $\nu = (u_x,-1)/\sqrt{1+u_x^2} = (\cos\theta, \sin\theta)$, $\tau = (\sin\theta, -\cos\theta)$, $\varkappa = \frac{u_{xx}}{(1+u_x^2)^{3/2}}$, $\gamma(\nu) = f(\theta)$ and using the homogeneity properties of γ one computes

$$f''(\theta) + f(\theta) = \langle\gamma''(\nu)\tau,\tau\rangle_{\mathbb{R}^2} = \gamma_{p_1p_1}(\cos\theta,\sin\theta)\frac{1}{\sin^2\theta} = \gamma_{p_1p_1}(u_x,-1)(1+u_x^2)^{3/2},$$

from which it follows

$$(f''(\theta)+f(\theta))\varkappa = g''(u_x)u_{xx}.$$

In particular (1.1_ε) can immediately be recovered (up to an obvious multiplication factor 1/2 for the Willmore term). ◇

6 Problems related to existence and convergence

In the following section we would like to shortly illustrate the problems that come up when we try to study the flow in the limit $\varepsilon \to 0$. The main question that motivates us is whether there is some sort of convergence, i.e. whether we can give a suitable notion of weak solution as ε goes to zero. A first step in this direction is to consider a weak formulation of the flow and derive energy estimates. In the following we outline the main ideas and give formal arguments but we do not go into any detail.

Roughly speaking, a weak formulation for the evolution equation reads: find $u^\epsilon \in W^{1,2}(0,T_\epsilon;H^2(0,1))$ such that $u^\varepsilon(0,t)=\alpha$, $u^\varepsilon(1,t)=\beta$ for all times t, $u^\varepsilon(\cdot,0)=u_0^\epsilon(\cdot)$, $\|u_0-u_0^\epsilon\|_{H^2(0,1)}\to 0$ for $\epsilon\to 0$, and

$$\int_0^1 \frac{u_t^\varepsilon}{\sqrt{1+(u_x^\varepsilon)^2}}\varphi\,dx = -\int_0^1 g'(u_x^\varepsilon)\varphi_x + \epsilon^2\left(2\frac{u_{xx}^\varepsilon\varphi_{xx}}{(1+(u_x^\varepsilon)^2)^{5/2}} - 5\frac{(u_{xx}^\varepsilon)^2u_x^\varepsilon\varphi_x}{(1+(u_x^\varepsilon)^2)^{7/2}}\right)dx \tag{6.1}$$

holds for all $\varphi\in H^2(0,1)\cap H_0^1(0,1)$ and for a.e. $t\in[0,T_\epsilon]$. Note that if a solution exists and it is smooth enough then it satisfies the natural boundary conditions.

Assuming short time existence for any ε and *assuming* that there exists a time T such that $u^\epsilon\in W^{1,2}(0,T;H^2(0,1))$ for all ϵ (here we are skipping a fair bit of work! At the time of writing the authors are not aware of short/long time existence results that precisely fit our setting), we can test with $\varphi=u_t^\epsilon$ and derive

$$\int_0^1 \frac{(u_t^\varepsilon)^2}{\sqrt{1+(u_x^\varepsilon)^2}}\,dx = -\int_0^1 g'(u_x^\varepsilon)u_{tx}^\varepsilon + \epsilon^2\left(2\frac{u_{xx}^\varepsilon u_{txx}^\varepsilon}{(1+(u_x^\varepsilon)^2)^{5/2}} - 5\frac{(u_{xx}^\varepsilon)^2u_x^\varepsilon u_{tx}^\varepsilon}{(1+(u_x^\varepsilon)^2)^{7/2}}\right)dx = -\frac{d}{dt}E_\varepsilon(u^\varepsilon).$$

Thus we immediately infer that there exists a constant C independent of t and ε such that for any $\varepsilon<1$ and $t\in(0,T)$ we have

$$\int_0^t\int_0^1 \frac{(u_t^\epsilon)^2}{\sqrt{1+(u_x^\varepsilon)^2}}\,dxdt + \sup_{(0,t)} E_\varepsilon(u^\epsilon)\le E_\epsilon(u_0^\epsilon)\le C. \tag{6.2}$$

From the above inequality and from the fact that $g(u_x^\varepsilon)\ge c_0\sqrt{1+(u_x^\varepsilon)^2}\ge c_0|u_x^\varepsilon|$ and $u^\varepsilon(x,t)=\alpha+\int_0^x u_x^\varepsilon(s,t)ds$ we infer that

$$\sup_{(0,T)}\|u^\varepsilon\|_{H^{1,1}(0,1)}\le C. \tag{6.3}$$

Next from $\int_0^t\int_0^1 \frac{(u_t^\epsilon)^2}{\sqrt{1+(u_x^\varepsilon)^2}}\,dxdt\le C$ and $\int_0^t\int_0^1 c_0\sqrt{1+(u_x^\varepsilon)^2}\,dxdt\le CT$ it follows that

$$2\sqrt{c_0}\int_0^t\int_0^1|u_t^\varepsilon|\,dxdt\le\int_0^t\int_0^1\frac{(u_t^\epsilon)^2}{\sqrt{1+(u_x^\varepsilon)^2}}+c_0\sqrt{1+(u_x^\varepsilon)^2}\,dxdt\le C(1+T)$$

and therefore

$$u_t^\varepsilon\in L^1(0,T;L^1(0,1)). \tag{6.4}$$

From (6.3) and (6.4) it follows that

$$u^\epsilon\in W^{1,1}((0,T)\times(0,1)). \tag{6.5}$$

This bound proves that a subsequence of u^ε converges in $L^1((0,T)\times(0,1))$ to a function $u\in L^1((0,T)\times(0,1))$. Unfortunately from the energy estimates alone we can not get any further information about the behaviour of u, in particular in relation to (6.1). Indeed, it is reasonable to expect that the above estimates plus a convexity condition on the map g should imply that the regularized ε-problem converges to the well defined anisotropic mean curvature flow as $\varepsilon\to 0$ (cf. [5]). However, this is not the case we are interested in, since for g uniformly convex and sufficiently smooth there is actually no need for regularization.

As shown in [4], where the authors thoroughly investigate a simplified model and put forward a number of conjectures, the limit problem is a very difficult one. Our hope is that the presence of a physically more consistent term such as the Willmore functional will help make its analysis more approachable – despite being more complicated at first sight.

To get first ideas of what phenomenon we should expect in the limit $\varepsilon \to 0$ it is useful to discretize the problem and perform some numerical simulations. A finite element discretization is discussed in Section 8 and first experiments are shown in Section 9.

7 The wrinkles phenomenon

Similarly to [4] (see also [15]) we have observed that the flow develops wrinkles very early in the stage of the evolution and that these wrinkles do not leave the region $\Sigma_L(u_0) := \{x \in [0,1] \,:\, u_{0x}(x) \in \mathrm{LUS}\}$, where u_0 is the given initial curve and

$$\mathrm{LUS} = \{y \in \mathbb{R} \,:\, g''(y) < 0\} \subseteq \mathrm{GUS} \tag{7.1}$$

(as defined in Section 2). In the following we try to give a plausible explanation for the phenomenon of wrinkles formation. The arguments are essentially given in [4, §4.1] but we repeat them here for the reader's convenience. We know that lines $\bar{u}(x) = px+q$, $x \in [0,1]$, $p, q \in \mathbb{R}$, are stationary solutions for the flow for any choice of ε (their stability or instability depending on the value p and the choice of anisotropy). We might therefore assume that, for perturbed initial data, say $\bar{u} + \delta\bar{v}(\cdot, \varepsilon)$, a solution to the flow is of type

$$u(x,t,\varepsilon;\delta) = \bar{u}(x) + \delta v(x,t,\varepsilon) + O(\delta^2)$$

for small δ. Plugging the above expression into (5.2), dividing by δ, and choosing $\delta = 0$, we observe that v has to satisfy the linear PDE

$$v_t = g''(p)v_{xx}\sqrt{1+p^2} - 2\varepsilon^2 \frac{v_{xxxx}}{(1+p^2)^2}.$$

We can solve this equation using the Ansatz $v(x,t,\varepsilon) = \psi(t,\varepsilon)\eta(x,\varepsilon)$. This gives

$$\frac{\psi_t}{\psi} = c(\varepsilon) = \frac{1}{\eta}(g''(p)\eta_{xx}\sqrt{1+p^2} - 2\varepsilon^2 \frac{\eta_{xxxx}}{(1+p^2)^2}).$$

Thus $\psi(t,\varepsilon) = \tilde{c}\exp(c(\varepsilon)t)$, and η is the solution of a fourth order linear ODE. The map η might be of different types depending on the values of $c(\varepsilon)$; however since we are interested in oscillating terms we might as well look directly for solutions of type $v(x,t,\varepsilon) = \exp(\lambda t)\sin(mx)$, where $\lambda = \lambda(\varepsilon)$, $m = m(\varepsilon)$. A straightforward computation gives that m and λ must satisfy the following relation

$$\lambda = -m^2\left(\frac{2\varepsilon^2}{(1+p^2)^2}m^2 + g''(p)\sqrt{1+p^2}\right).$$

Thus we see that if g is convex then λ is negative and oscillations can be basically neglected. On the contrary, if $g''(p) < 0$ then we see that λ is positive provided that $m^2 < -\frac{g''(p)}{2\varepsilon^2}(1+p^2)^{5/2}$. More precisely λ assumes it maximum value

$$\lambda_{max} = \frac{(g''(p))^2}{8\varepsilon^2}(1+p^2)^3 \tag{7.2}$$

at $m_{max}^2 = -\frac{g''(p)}{4\varepsilon^2}(1+p^2)^{5/2}$. This value can be very large when ε is small.

Next, thinking of a flow with initial curve u_0, we can expect that locally around $x_0 \in [0,1]$ the initial map can be approximated by its linear part $u_{0x}(x_0)(x-x_0)+u_0(x_0)$. Assuming that the above analysis applies then we expect the wrinkles phenomenon to appear only in the region $\Sigma_L(u_0) = \{x \in [0,1] : u_{0x}(x) \in \mathrm{LUS}\}$ as stated above. Furthermore the expression for m_{max} suggests that the wave length of the appearing wrinkles should be $O(\varepsilon)$.

8 Discretization

To discretize the problem we compute the first variation of the functional E_ε using the ideas proposed in [14]. One advantage in doing so is that it is rather easy to show that in the semi-discrete setting the energy decreases along the flow. We introduce a new variable $w := \varkappa\sqrt{1+u_x^2} = \frac{u_{xx}}{1+u_x^2}$. For variations of type $u+\delta\varphi$, where u is as smooth as required and satisfies the natural boundary conditions, and $\varphi \in C_0^\infty(I)$, $I=(0,1)$, we have that

$$\int_I \frac{w_\delta}{\sqrt{1+(u_x+\delta\varphi_x)^2}}\psi\,dx = -\int_I \frac{u_x+\delta\varphi_x}{\sqrt{1+(u_x+\delta\varphi_x)^2}}\psi_x\,dx$$

holds for all $\psi \in C_0^\infty(I)$. Derivation with respect to δ yields

$$\int_I \frac{d}{d\delta}\Big|_{\delta=0} w_\delta \frac{\psi}{\sqrt{1+u_x^2}}\,dx = \int_I w\psi\frac{u_x\varphi_x}{(1+u_x^2)^{3/2}} - \frac{\psi_x\varphi_x}{(1+u_x^2)^{3/2}}\,dx. \tag{8.1}$$

In particular this equation holds for $\psi = w$. Using this fact we compute

$$\begin{aligned}
\frac{d}{d\delta}\Big|_{\delta=0} E_\varepsilon(u+\delta\varphi) &= \frac{d}{d\delta}\Big|_{\delta=0}\left(\int_I g(u_x+\delta\varphi_x) + \varepsilon^2\frac{w_\delta^2}{\sqrt{1+(u_x+\delta\varphi_x)^2}}\,dx\right)\\
&= \int_I g'(u_x)\varphi_x + 2\varepsilon^2\frac{d}{d\delta}\Big|_{\delta=0} w_\delta\frac{w}{\sqrt{1+u_x^2}} - \varepsilon^2 w^2\frac{u_x\varphi_x}{(1+u_x^2)^{3/2}}\,dx\\
&= \int_I g'(u_x)\varphi_x + \varepsilon^2 w^2\frac{u_x\varphi_x}{(1+u_x^2)^{3/2}} - 2\varepsilon^2\frac{w_x\varphi_x}{(1+u_x^2)^{3/2}}\,dx.
\end{aligned}$$

Thus we can reformulate our original ε-problem as follows: we look for $u(\cdot,t) \in H^{1,2}(I)$ and $w(\cdot,t) \in H_0^{1,2}(I)$ such that $u_t(\cdot,t) \in H^{1,2}(I)$, $u(0,t)=\alpha$, $u(1,t)=\beta$, $u(\cdot,0)=u_0$, and

$$\int_I \frac{u_t}{\sqrt{1+u_x^2}}\varphi\,dx = -\int_I g'(u_x)\varphi_x + \varepsilon^2 w^2\frac{u_x\varphi_x}{(1+u_x^2)^{3/2}} - 2\varepsilon^2\frac{w_x\varphi_x}{(1+u_x^2)^{3/2}}\,dx \quad \forall\varphi \in H_0^{1,2}(I), \tag{8.2}$$

$$\int_I \frac{w}{\sqrt{1+u_x^2}}\psi\,dx = -\int_I \frac{u_x}{\sqrt{1+u_x^2}}\psi_x\,dx \qquad \forall\psi \in H_0^{1,2}(I) \tag{8.3}$$

for almost every time $t \in [0, T_\varepsilon]$. Note that by choosing $\varepsilon = 1$ and leaving out the term involving the map g we recover the one-dimensional version of the scheme given in [11].

Differentiating (8.3) with respect to time we obtain an equation which we refer to as $(8.3)_t$. Testing with $\psi = w$ in $(8.3)_t$ and $\varphi = u_t$ in (8.2) we immediately infer

$$\frac{d}{dt}E_\varepsilon(u) = -\int_I \frac{u_t^2}{\sqrt{1+u_x^2}} \le 0. \tag{8.4}$$

Now let $\bar{I} = \bigcup_{j=1}^{N+1} I_j$ be a decomposition of the interval $\bar{I} = [0,1]$ into intervals $I_j = [x_{j-1}, x_j]$ for $j = 1, \dots, N+1$. We set $x_0 = 0$ and $x_{N+1} = 1$. Let $h_j = |I_j|$ and $h = \max_{j=1,\dots,N+1} h_j$ be the maximal diameter of a grid element. We assume that for some constant $\tilde{c} > 0$ we have that $h_j \ge \tilde{c}h$. In practice we will use equidistant grid points so that $h = h_j$ for all $j = 1, \dots, N+1$. We introduce the finite dimensional space

$$X_h := \{v \in C^0(\bar{I}, \mathbb{R}) \,:\, v|_{I_j} \in P_1(\bar{I}_j),\ j = 1, \cdots, N+1\}$$

of continuous piecewise affine functions on the grid. The $N+2$ scalar nodal basis functions $\varphi_j \in X_h$ are defined by $\varphi_j(x_i) = \delta_{ij}$. Let $X_h^0 := \operatorname{span}\{\varphi_1, \dots, \varphi_N\}$ and I_h be the usual linear interpolation operator.

The semi-discrete problem reads: find $u_h(\cdot,t) \in X_h$, $w_h(\cdot,t) \in X_h^0$, such that $u_h(0,t) = \alpha$, $u_h(1,t) = \beta$, $u_h(\cdot,0) = I_h u_0$ and

$$\int_I \frac{u_{ht}}{\sqrt{1+u_{hx}^2}}\varphi_h\,dx = -\int_I g'(u_{hx})\varphi_{hx} + \varepsilon^2 w_h^2 \frac{u_{hx}\varphi_{hx}}{(1+u_{hx}^2)^{3/2}} - 2\varepsilon^2 \frac{w_{hx}\varphi_{hx}}{(1+u_{hx}^2)^{3/2}}\,dx \quad \forall \varphi_h \in X_h^0, \tag{8.5}$$

$$\int_I \frac{w_h}{\sqrt{1+u_{hx}^2}}\psi_h\,dx = -\int_I \frac{u_{hx}}{\sqrt{1+u_{hx}^2}}\psi_{hx}\,dx \qquad \forall \psi_h \in X_h^0\,. \tag{8.6}$$

Note that because no integration by parts was used in the derivation of the first variation a discrete analogue of (8.4) can immediately be obtained also for the semi-discrete problem.

For the time discretization we follow ideas given in [11] and provide a semi-implicit scheme. Let τ be the time step. For a generic function f we denote its evaluation at the m-th time level $t^m = m\tau$ by $f^m = f(\cdot, t^m)$. The discrete problem can be formulated as follows: compute $u_h^{m+1} \in X_h$ and $w_h^{m+1} \in X_h^0$ so that $u_h^{m+1}(0) = \alpha$, $u_h^{m+1}(1) = \beta$ and

$$\begin{aligned}\int_I \frac{u_h^{m+1} - u_h^m}{\tau}\frac{\varphi_h}{Q_h^m} + \int_I g'(u_{hx}^m)\varphi_{hx} \\ + \varepsilon^2 \int_I \frac{(w_h^m)^2}{(Q_h^m)^3} u_{hx}^{m+1}\varphi_{hx} - 2\varepsilon^2 \int_I \frac{w_{hx}^{m+1}}{(Q_h^m)^3}\varphi_{hx} = 0 \quad \forall \varphi_h \in X_h^0\end{aligned} \tag{8.7}$$

and

$$\int_I \frac{w_h^{m+1}}{Q_h^m}\psi_h + \int_I \frac{u_{hx}^{m+1}}{Q_h^m}\psi_{hx} = 0 \qquad \forall \psi_h \in X_h^0\,, \tag{8.8}$$

where $Q_h^m = \sqrt{1+(u_{hx}^m)^2}$.

As initial data we use $u_h^0 = I_h u_0$ and w_h^0, which is computed from

$$\int_I \frac{w_h^0}{Q_h^0}\psi_h + \int_I \frac{u_{hx}^0}{Q_h^0}\psi_{hx} = 0 \qquad \forall \psi_h \in X_h^0\,.$$

By using the expansions

$$u_h^m = \sum_{j=1}^{N} U_j^m \varphi_j + \alpha\varphi_0 + \beta\varphi_{N+1}, \qquad w_h^m = \sum_{j=1}^{N} W_j^m \varphi_j$$

and setting $U^m = (U_1^m, \dots, U_N^m)$, $W^m = (W_1^m, \dots, W_N^m)$, as well as

$$M_{ij}^m = \int_I \frac{\varphi_i \varphi_j}{Q_h^m}, \qquad E_{ij}^m = \int_I \frac{\varphi_{ix}\varphi_{jx}}{(Q_h^m)^3}, \qquad A_{ij}^m = \int_I \frac{\varphi_{ix}\varphi_{jx}}{Q_h^m}, \qquad B_{ij}^m = \int_I \frac{(w_h^m)^2}{(Q_h^m)^3}\varphi_{ix}\varphi_{jx},$$

we can write the linear systems (8.7) and (8.8) in the form

$$\frac{1}{\tau} M^m (U^{m+1} - U^m) + \varepsilon^2 B^m U^{m+1} - 2\varepsilon^2 E^m W^{m+1} = R_u^m \tag{8.9}$$

$$M^m W^{m+1} + A^m U^{m+1} = R_w^m, \tag{8.10}$$

where for h sufficiently small we have that

$$R_u^m = \begin{pmatrix} -\int_I g'(u_{hx}^m)\varphi_{1x} - \varepsilon^2\alpha \int_I \frac{(w_h^m)^2}{(Q_h^m)^3}\varphi_{0x}\varphi_{1x} \\ \vdots \\ -\int_I g'(u_{hx}^m)\varphi_{jx} \\ \vdots \\ -\int_I g'(u_{hx}^m)\varphi_{Nx} - \varepsilon^2\beta \int_I \frac{(w_h^m)^2}{(Q_h^m)^3}\varphi_{(N+1)x}\varphi_{Nx} \end{pmatrix}, \qquad R_w^m = \begin{pmatrix} -\alpha \int_I \frac{\varphi_{0x}\varphi_{1x}}{Q_h^m} \\ 0 \\ \vdots \\ 0 \\ -\beta \int_I \frac{\varphi_{(N+1)x}\varphi_{Nx}}{Q_h^m} \end{pmatrix}.$$

Thus we need to compute

$$\left(\frac{1}{\tau} M^m + \varepsilon^2 B^m + 2\varepsilon^2 E^m (M^m)^{-1} A^m\right) U^{m+1} = \frac{1}{\tau} M^m U^m + 2\varepsilon^2 E^m (M^m)^{-1} R_w^m + R_u^m. \tag{8.11}$$

We solve this system by a conjugate gradient method. In the practical computations we replace $(M^m)^{-1}$ with the inverse of the diagonal matrix $\tilde{M}^m$ which is obtained from M^m by mass lumping.

In practice stability issues can be overcome by choosing $\tau \le ch^2$ and $\varepsilon \le ch$. For the case that we do not wish to couple ε and h, and still have a time step restriction of type $\tau \le ch^2$, it is essential to choose "good" initial data.

9 Numerical simulations

In the following we describe the anisotropy functions that have been used for the numerical simulations.

9.1 A one-parameter family of anisotropies

The boundary of the Frank diagram $\partial\mathcal{F}_a := \{\xi \in \mathbb{R}^2 : \gamma(\xi) = 1\}$ is described parametrically by $\gamma(f(\theta)\cos\theta, f(\theta)\sin\theta) = 1$ where

$$f(\theta) = 4 - a\sin^2(\theta), \qquad \theta \in [0, 2\pi], \quad a \in [0, 4).$$

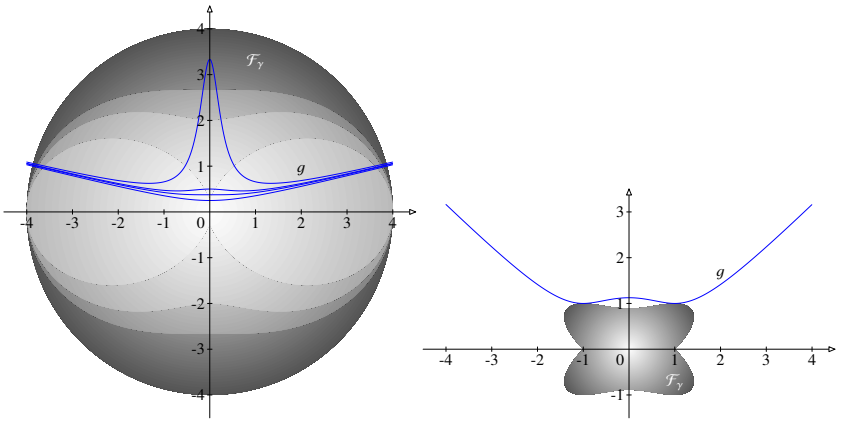

Figure 4: Frank diagram and plot of the map g for the anisotropy discussed in Subsection 9.1 (left) for $a = 0, 4/3, 2, 3.7$ and Subsection 9.2 (right)

We will show below that for $a \leq 4/3$ the Frank diagram is convex, thus we will be interested in the anisotropies with $a \in (4/3, 4)$. From $\gamma(\cos\theta, \sin\theta) \overset{(2.6)}{=} \frac{1}{f(\theta)}$ and $\frac{y}{\sqrt{y^2+1}} = \cos\theta$, $-\frac{1}{\sqrt{y^2+1}} = \sin\theta$ for $\theta \in (\pi, 2\pi)$, we deduce that for $y \in \mathbb{R}$ the map g is given by

$$g(y) = \sqrt{y^2+1}\,\gamma\left(\frac{y}{\sqrt{y^2+1}}, -\frac{1}{\sqrt{y^2+1}}\right) \overset{(2.6)}{=} \frac{\sqrt{y^2+1}}{f(\theta)} = \frac{(y^2+1)^{3/2}}{4y^2+4-a}.$$

In Figure 4 (left) we show a plot for the Frank diagram and the map g for different values of a. A straightforward calculation gives

$$g'(y) = \frac{3y\sqrt{y^2+1}}{4(y^2+1)-a} - \frac{8y(y^2+1)^{3/2}}{(4(y^2+1)-a)^2} = \frac{4y(y^2+1)^{3/2} - 3ay\sqrt{y^2+1}}{(4(y^2+1)-a)^2},$$

therefore we infer that

$$\text{for } a \in [0, 4/3] : \qquad g'(y) = 0 \text{ iff } y = 0,$$

$$\text{for } a \in (4/3, 4) : \qquad g'(y) = 0 \text{ iff } y = 0 \text{ or } y_{\pm G} := \pm\sqrt{\frac{3}{4}a - 1}.$$

We have that $g(0) = \frac{1}{4-a}$ and $g(y_\pm) = \frac{\left(\frac{3}{4}a\right)^{3/2}}{2a}$. Further one calculates that

$$g''(y) = \frac{8(a+2)y^4 + 2y^2(3a^2-4a+16) + (4-a)(4-3a)}{(4(y^2+1)-a)^3\sqrt{y^2+1}}.$$

Note that $3a^2-4a+16 \geq 0$ for all $a \in \mathbb{R}$. Moreover $a+2 \geq 0$ for $0 \leq a < 4$. For $a \leq 4/3$ it is obviously $g''(y) \geq 0$ for all $y \in \mathbb{R}$. For $a \in (4/3, 4)$ we have that $(4-a)(4-3a) < 0$, and therefore the solutions of $g''(y) = 0$ are given by

$$y_{\pm L} := \pm\sqrt{\frac{-(3a^2-4a+16) + \sqrt{(3a^2-4a+16)^2 - 8(a+2)(4-a)(4-3a)}}{8(a+2)}}.$$

In particular $g''(y) \leq 0$ for $y \in [y_L, y_L]$. Note that for $a \in (4/3, 4)$, we have that LUS $= (-y_L, y_L)$ and GUS $= (-y_G, y_G)$.

9.2 A non-convex anisotropy with minima in ±1

Sometimes it is convenient to have an anisotropy function g that takes its minima at prescribed values, for instance at $y = \pm 1$. Define

$$g(y) = \begin{cases} \frac{1}{8}(y-1)^2(y+1)^2 + 1, & |y| \le 1 \\ \sqrt{1 + (|y|-1)^2}, & |y| > 1 \end{cases}$$

Indeed $g(y) = 1$ if and only if $y = \pm 1$. A straightforward computation gives

$$g'(y) = \begin{cases} \frac{1}{2}y(y^2-1), & |y| < 1 \\ \frac{(|y|-1)}{\sqrt{1+(|y|-1)^2}} sgn(y), & |y| > 1 \end{cases} \qquad g''(y) = \begin{cases} \frac{1}{2}(3y^2-1), & |y| < 1 \\ \frac{1}{(1+(|y|-1)^2)^{3/2}}, & |y| > 1 \end{cases}.$$

Note that $g \in C^2(\mathbb{R})$, and $g''(y) = 0$ if and only if $y = \pm\frac{1}{\sqrt{3}}$. Thus we have that

$$\text{LUS} = \left(-\frac{1}{\sqrt{3}}, \frac{1}{\sqrt{3}}\right), \qquad \text{GUS} = (-1, 1).$$

Now we construct the associated map γ. Using the fact that γ should be homogeneous of degree one we deduce that for $x \in \mathbb{R}$ and $y < 0$ the map γ is given by $\gamma(x, y) = -yg\left(-\frac{x}{y}\right)$. For $x \in \mathbb{R}$ and $y > 0$ set $\gamma(x, y) := \gamma(x, -y)$. Finally $\gamma(\pm 1, 0) := \lim_{z\to\pm\infty} \frac{g(z)}{\sqrt{1+z^2}} = 1$, thus $\gamma(x, 0) = |x|$. Summing up we have that

$$\begin{aligned} x \in \mathbb{R},\ y < 0 :&\quad \gamma(x, y) = \begin{cases} -\frac{1}{8}y\left(\frac{x}{y}+1\right)^2\left(\frac{x}{y}-1\right)^2 - y, & \left|\frac{x}{y}\right| \le 1 \\ -y\sqrt{1 + (|\frac{x}{y}|-1)^2}, & \left|\frac{x}{y}\right| > 1 \end{cases} \\ x \in \mathbb{R},\ y = 0 :&\quad \gamma(x, y) = |x| \\ x \in \mathbb{R},\ y > 0 :&\quad \gamma(x, y) = \gamma(x, -y). \end{aligned}$$

One can verify that γ is continuous on $\mathbb{R}^2$ and homogeneous of degree one. Moreover $\gamma \in C^2(\mathbb{R}^2 \setminus \{0\} \cap \{(x, y) \in \mathbb{R}^2 : y \le 0\})$. A plot for γ and g is given in Figure 4 (right).

9.3 Numerical experiments

Next we describe some of the experiments that we have performed.

Test 1 - Anisotropic Mean Curvature Flow We choose the initial curve to be

$$u_0(x) = x^2 + 0.6x, \qquad x \in [0, 1],$$

and let it develop solely by anisotropic mean curvature (therefore we set $\varepsilon = 0$) with Dirichlet boundary conditions. The anisotropy function chosen is the one described in Section 9.2. Since $u_{0x}(x) \in \mathbb{R} \setminus \text{LUS}$ for all $x \in [0, 1]$ we expect a forward parabolic behaviour. Indeed the curve straightens up to a line, which is a steady state. To avoid stability issues we chose $\tau = h^3/2$.

Test 2 - First formation of wrinkles If

$$\Sigma_L(u_0) = \{x \in [0, 1] : u_{0x}(x) \in \text{LUS}\} \neq \emptyset$$

then formation of wrinkles is expected (see Section 7) and in fact it is also experimentally observed. This phenomenon is characterized by a rather drastic drop in the

energy and by the fact that wrinkles appear and are never observed to leave the region $\Sigma_L(u_0)$. In the following we show results for different choices of anisotropy functions and initial curves.

Test 2a Here we experiment with the anisotropy function given in Section 9.2, for which LUS $= \left(-1/\sqrt{3}, 1/\sqrt{3}\right)$. Similarly to [4, § 6.2] we choose the initial curve to be

$$u_0(x) = \frac{1}{4}\sin(2\pi x) + \frac{\pi}{2}x, \qquad x \in [0,1]. \tag{9.1}$$

A plot for u_0 is given in Figure 15 (left). A straightforward calculation gives $\Sigma_L(u_0) = (x_L, 1 - x_L)$, where $x_L = \frac{1}{2\pi}\arccos(\frac{2}{\pi\sqrt{3}} - 1) \simeq 0.3589748$. We choose time step $\tau = h^2/100$ and $\varepsilon = 10^{-4}$, where $h = 10^{-3}$. In the three shots of Figure 5 we zoom on the evolution of the first wrinkles at the times $t = 6.42 \times 10^{-6}$, $t = 1.642 \times 10^{-5}$, $t = 9.445 \times 10^{-5}$; the horizontal bar indicates the region $\Sigma_L(u_0)$.

Test 2b For the next test we choose again the initial curve (9.1), the anisotropy from Section 9.2, $\tau = h^2/100$, where $h = 10^{-3}/8$, and $\varepsilon = 1.25 \cdot 10^{-7}$. We show the evolution in Figure 6 (left). Compared to Test 2a, where (the grid size h and) the parameter ε is not as fine as in this case, we observe that the oscillations strongly intensify. In view of the expected wavelength of size $O(\varepsilon)$ (see Section 7) this is actually not surprising. Finally in Figure 7 we zoom on a wrinkle at time $t = 1.5620313 \cdot 10^{-6}$ and observe that the slope is basically ± 1.

Test 2c Here we choose the anisotropy function described in Section 9.1 with $a = 3.7$. In this case LUS $\simeq (-0.15767616, 0.15767616)$, GUS $\simeq (-1.33229126, 1.33229126)$. As a start function we have chosen the map (see Figure 8 (left))

$$u_0(x) = 3x^5 - 8x^4 + 6x^3, \qquad x \in [0,1],$$

for which we have that $\Sigma_L(u_0) \simeq [0, 0.1029975194)$. For this experiment we set $\tau = h^3/10$ and $\varepsilon = 10^{-4}$, where $h = 10^{-3}$. In Figure 9 we observe how the wrinkles invade $\Sigma_L(u_0)$. A plot for the energy E_ε in dependence of time is given in Figure 8 (right). Note that for a discrete curve u_h^m the energy in practice is calculated by

$$E_\varepsilon(u_h^m) = \int_I g(u_{hx}^m)\,\mathrm{d}x + \varepsilon^2 \int_I \frac{(w_h^m)^2}{\sqrt{1 + (u_{hx}^m)^2}}\,dx.$$

Test 3 - Discontinuity of the energy at $t = 0$ Next we want to investigate the behaviour of the flow at initial times and for $\varepsilon \to 0$. Similarly to [4, § 6.2] we compute the quantities

$$\begin{aligned} t &\mapsto E_\varepsilon(u_h^\varepsilon(\cdot,t)) \\ t &\mapsto d^\varepsilon(t) := \frac{\|u_0 - u_h^\varepsilon(\cdot,t)\|_{L^2(0,1)}}{\|u_0\|_{L^2(0,1)}}, \\ t &\mapsto f^\varepsilon(t) := 1 - \frac{E_\varepsilon(u_h^\varepsilon(\cdot,t))}{E_\varepsilon(u_{0h})}. \end{aligned}$$

for $\varepsilon \to 0$. In [4, § 6.4] the authors perform this test using an anisotropy function similar to the one depicted in Section 9.2 and initial curve $u_0(x) = x/2$. This curve is

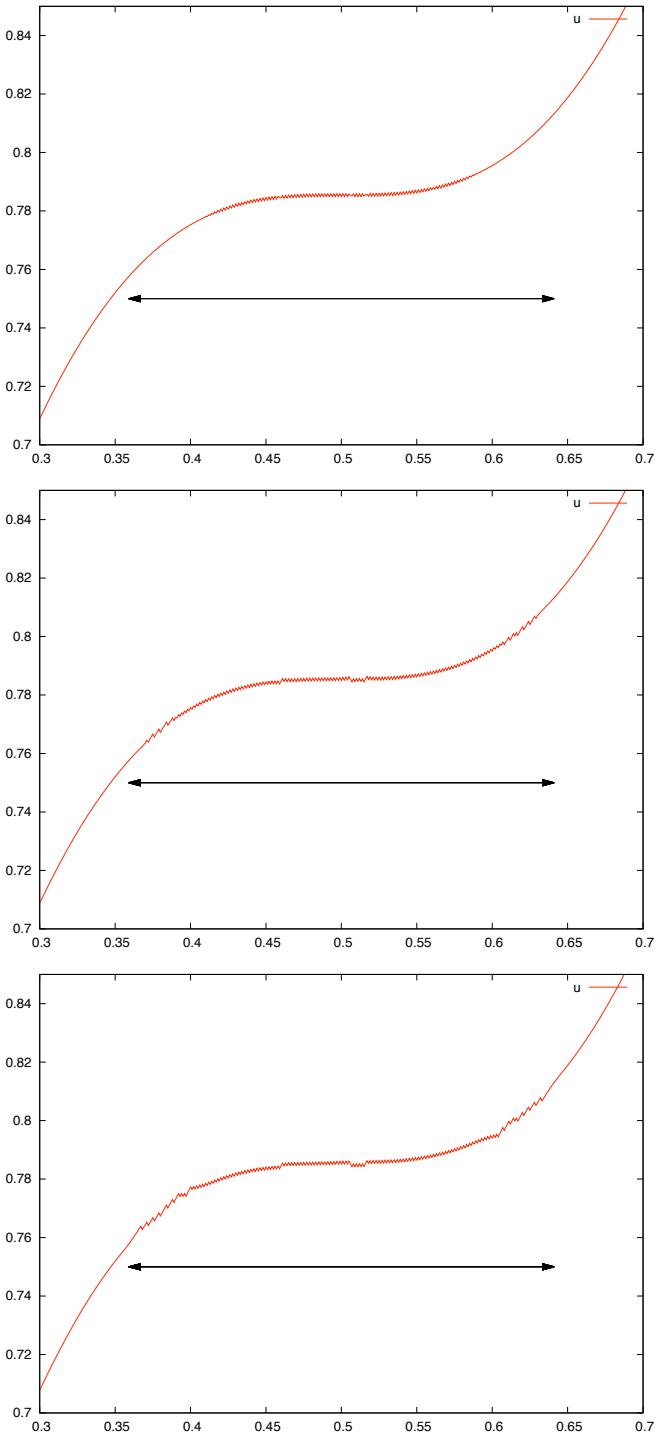

Figure 5: Test 2a - Evolution at time $t = 6.42 \times 10^{-6}$, $t = 1.642 \times 10^{-5}$, $t = 9.445 \times 10^{-5}$ (from the top to the bottom); the horizontal bar indicates the region $\Sigma_L(u_0)$.

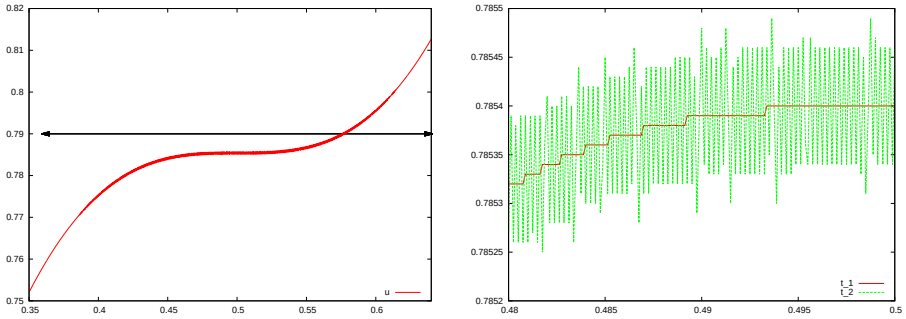

Figure 6: Test 2b - Evolution at time $t = 1.09375 \cdot 10^{-7}$ (left). Zoom on the evolution at times $t_1 = 0.78125 \cdot 10^{-8}$ and $t_2 = 1.09375 \cdot 10^{-7}$ (right).

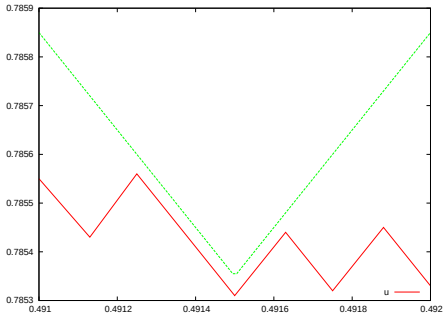

Figure 7: Test 2b - Evolution at time $t = 1.5620313 \cdot 10^{-6}$. A v-shaped line with slope ± 1 is also represented.

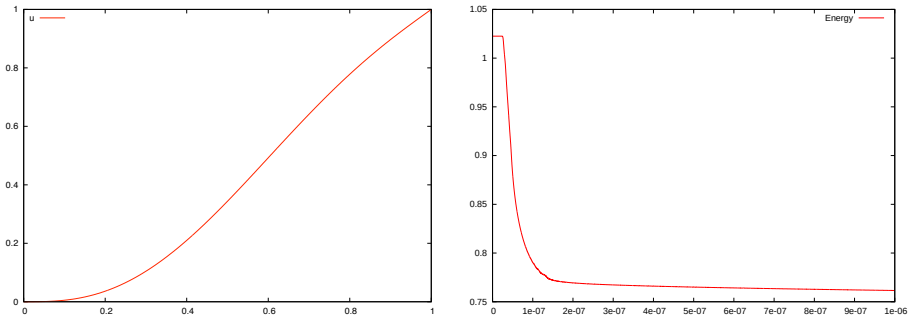

Figure 8: Test 2c - Initial curve (left); energy decrease along the flow (right).

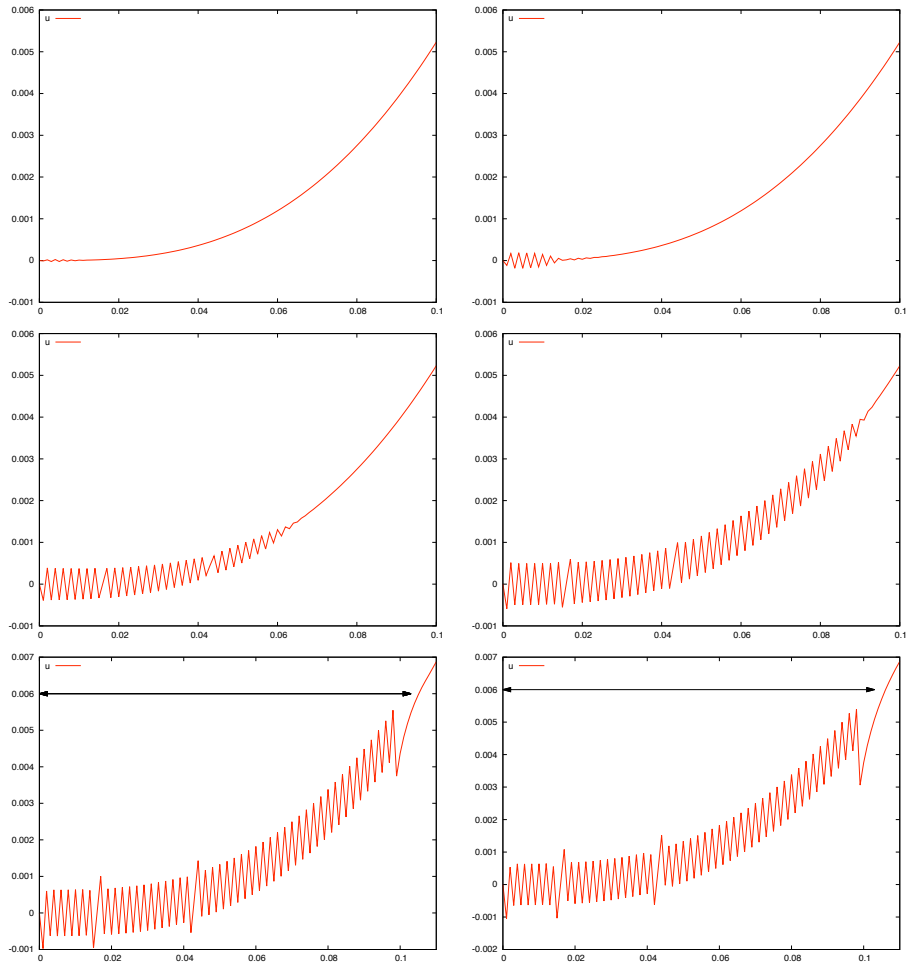

Figure 9: Test 2c - Evolution at times $t = 2.5 \cdot 10^{-8}$, $t = 3 \cdot 10^{-8}$, $t = 5 \cdot 10^{-8}$, $t = 9 \cdot 10^{-8}$, $t = 5.2 \cdot 10^{-7}$, $t = 9.948 \cdot 10^{-7}$. The horizontal bar indicates the region $\Sigma_L(u_0)$.

a stationary unstable solution for the flow. The authors explain that despite this fact they observe (numerically) the wrinkles phenomenon and that the latter is probably induced by round-off errors and the instability property of the initial map. With our discretization (and anisotropy from Section 9.2) the map $u_0(x) = x/2$ is stationary also in the discrete setting.

For the next experiments we choose the initial curve

$$u_0(x) = \frac{\sin(2\pi x)}{20\pi}, \qquad x \in [0, 1], \tag{9.2}$$

and the anisotropy function given in Section 9.2. For fixed time step $\tau = 10^{-10}$ and $h = 10^{-3}$ we test for

$$\varepsilon_1 = 2 \cdot 10^{-3}, \qquad \varepsilon_2 = 10^{-3}, \qquad \varepsilon_3 = \frac{1}{2} \cdot 10^{-3}.$$

Note that $\Sigma_L(u_0) = [0, 1]$ and, as expected, wrinkles develop in the whole domain. A plot of the evolution for ε_1 is given in Figure 10. A plot for E_ε, f^ε, and d^ε for the above choices of ε is shown in Figure 11. A comparison of the plots presented in Figure 11 shows that the rapid decrease in the energy takes place closer and closer to the origin when $\varepsilon \to 0$. This induces us to believe that as ε approaches zero there should be some sort of discontinuity of the energy at $t = 0$. In Figure 12 the plot of the map $\varepsilon \mapsto T(\varepsilon)$, where $T(\varepsilon)$ denotes the time at which the energy E_ε starts to drop, suggests that $T(\varepsilon) \simeq c\varepsilon^2$ (the values for $T(\varepsilon)$ are read from Figure 11). These facts have already been observed in [4] (see also [4, Conjecture 4.1]).

Test 4 - Resolution of wrinkles With the next experiment we want to show that for a fixed $\varepsilon > 0$ a definite number of wrinkles is to be expected and that the resolution of the wrinkles improves by letting $h \to 0$. Indeed, following the discussion on the wrinkle phenomenon in Section 7, we expect the wavelength l of a point $y \in \Sigma_L(u_0)$ to be something like

$$l(y) = \frac{4\varepsilon\pi}{\sqrt{-g''(y)(1 + y^2)^{5/2}}}.$$

For the initial curve (9.2), $\varepsilon = \frac{10^{-3}}{2}$, and the anisotropy function given in Section 9.2, the theoretically predicted number of wrinkles is approximately 112. For time step $\tau = \frac{h^2}{10^4}$ and grid size $h_1 = 10^{-3}$ and $h_2 = \frac{1}{2}10^{-3}$, we count 116 and 115 wrinkles respectively (at time $t = 0.0003$). In Figure 13 we show the evolution at $t = 0.0003$, a time for which wrinkles have already invaded the whole region. Notice the improved wrinkles resolution for h_2.

Test 5 - Wavelength Following the above considerations on the wavelength of the wrinkles, we expect the number of wrinkles to double whenever we halve the value of ε. In Figure 14 we show that this is exactly the case. For this experiment we have chosen the same initial curve, anisotropy, time step, ε, and grid size as in Test 3.

Test 6 - Long time computation Here we show the long time computation for Test 2a. In Figure 15 we observe that the flow develops as expected towards a line (a minimum for the energy E_ε). In Figure 16 we show another two details of the evolution showing the shrinking of the wrinkled region.

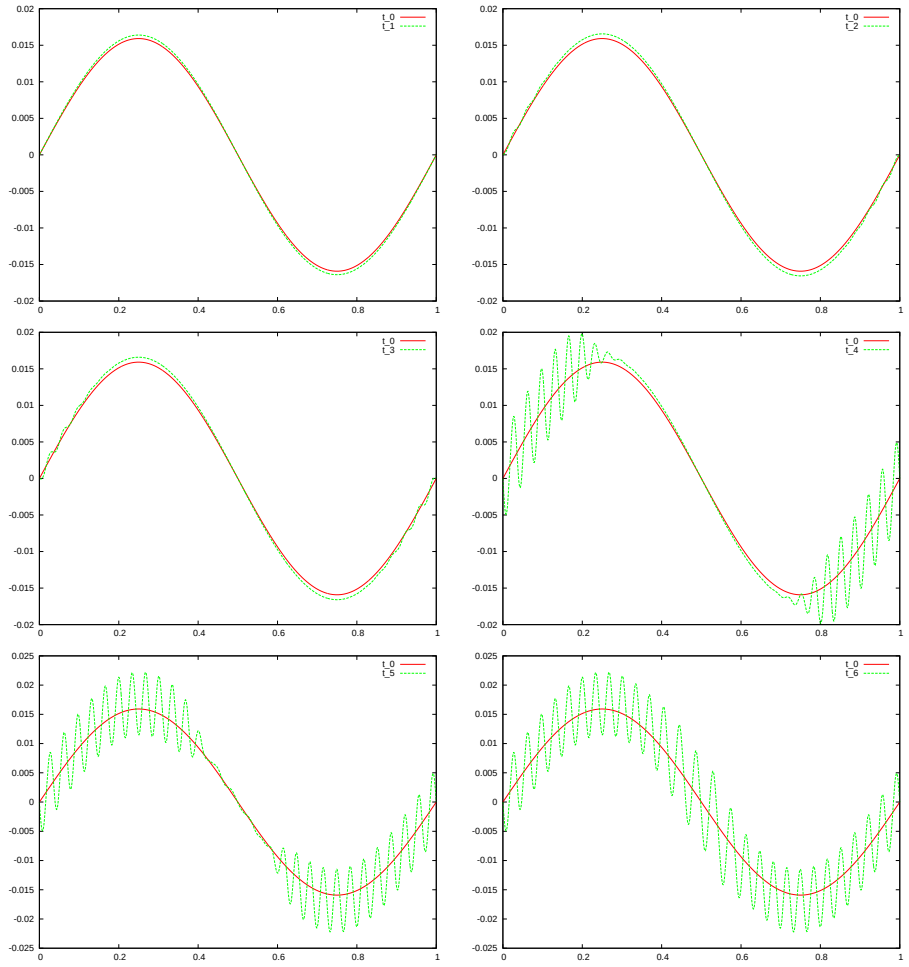

Figure 10: Test 3 - Evolution for $\varepsilon = 2 \cdot 10^{-3}$ at times $t_0 = 0$ and $t_1 = 0.0015$, $t_2 = 0.002$, $t_3 = 0.0021$, $t_4 = 0.0028$, $t_5 = 0.0036$, $t_6 = 0.0059$.

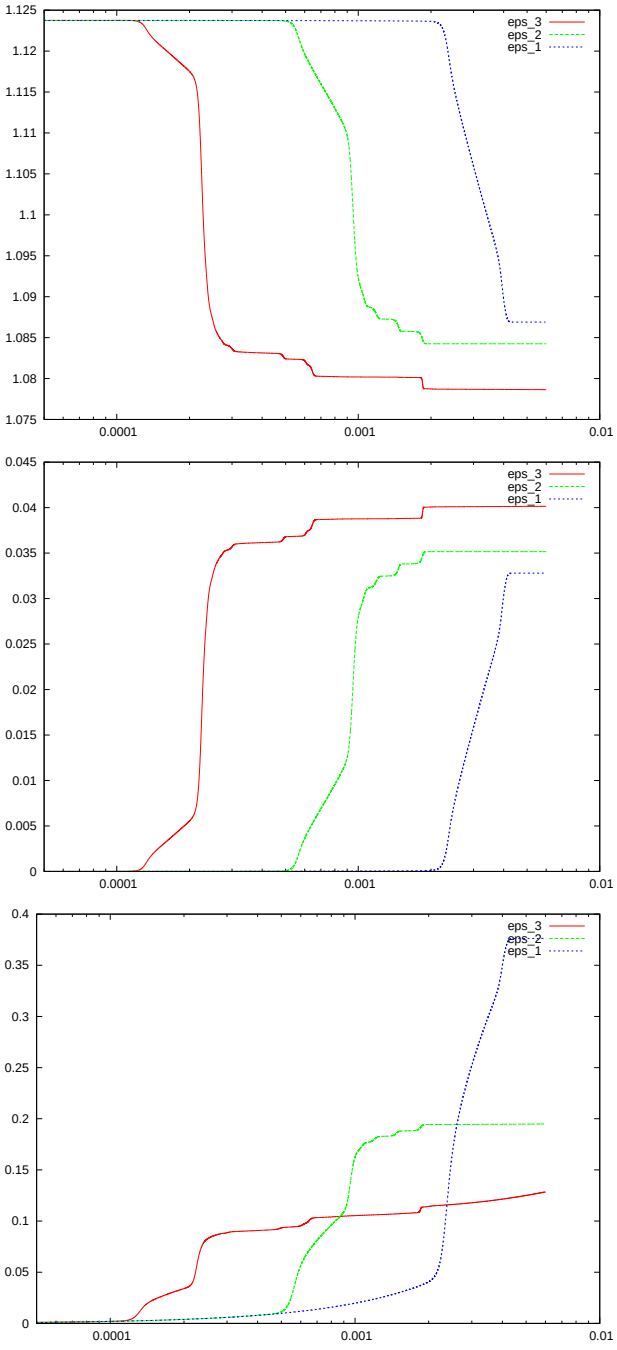

Figure 11: Test 3 - For the choices of $\varepsilon_1 = 2 \cdot 10^{-3}$, $\varepsilon_2 = 10^{-3}$, $\varepsilon_3 = \frac{1}{2} \cdot 10^{-3}$ we show the evolution of E_ε, f^ε, and d^ε (from top to bottom). A logarithmic scale is used for the time axis.

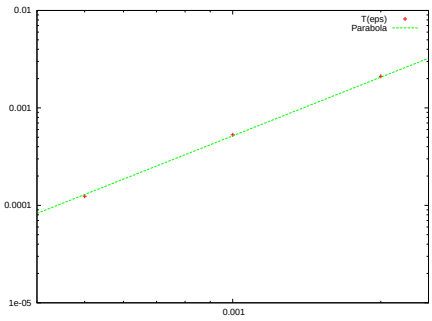

Figure 12: Test 3 - Plot of the function $\varepsilon \to T(\varepsilon)$ against the parabola $517 \cdot x^2$ in logarithmic scale.

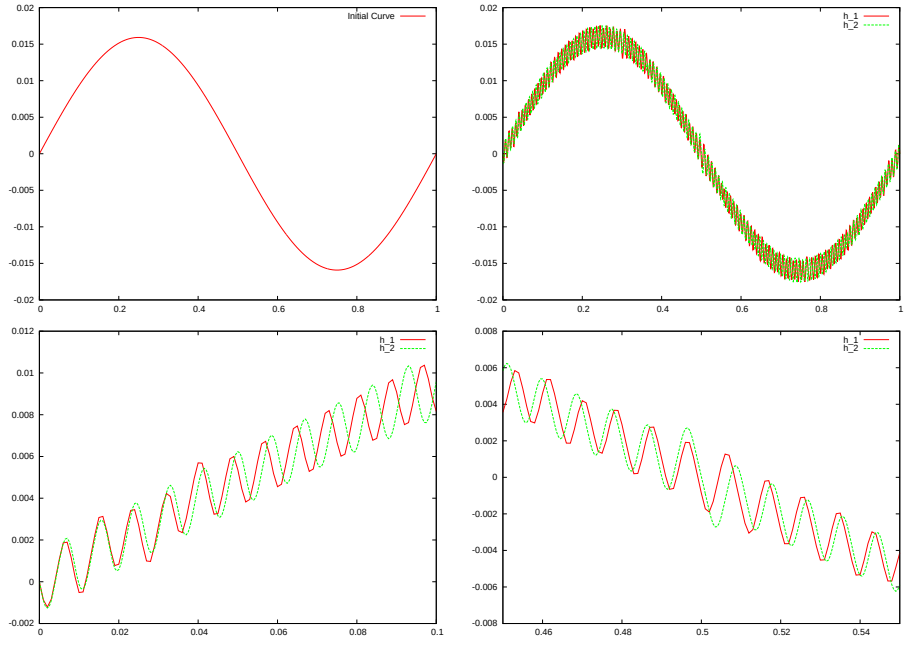

Figure 13: Test 4 - First row: Initial curve and evolution at time $t = 0.0003$, for $h_1 = 10^{-3}$, $h_2 = \frac{1}{2}10^{-3}$. Second row: two details of the right figure in the first row.

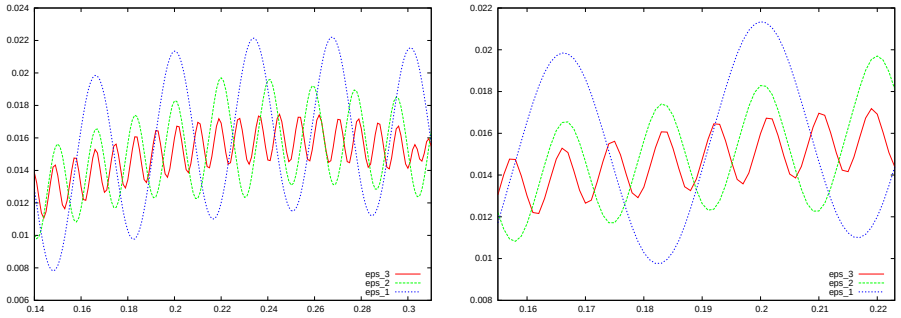

Figure 14: Test 5 - For the choices of $\varepsilon_1 = 2 \cdot 10^{-3}$, $\varepsilon_2 = 10^{-3}$, $\varepsilon_3 = \frac{1}{2} \cdot 10^{-3}$ we show the evolution in the interval $[0.14, 0.31]$ at time $t_1 = 0.0044$, $t_2 = 0.0014401$, and $t = 0.0002509$ respectively. The times are chosen so that for all three experiments the discrete energy E_ε equals approximately 1.08689 (cf. the plot of the Energy E_ε in Figure 11) and wrinkles have fully developed in the region considered. A zoom is presented in the right figure.

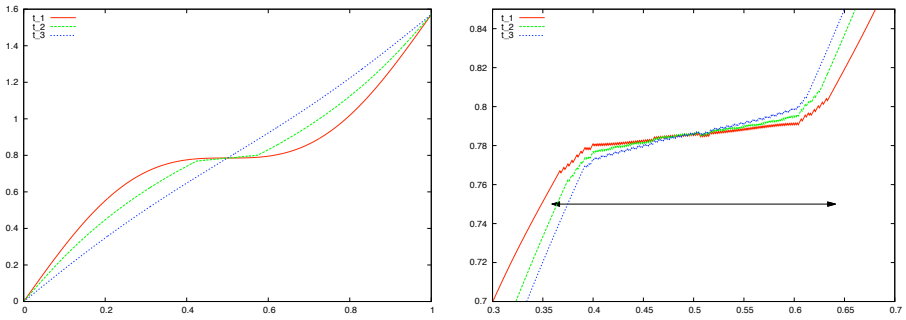

Figure 15: Test 6 (Test 2a) - Flow at times $t_1 = 0$, $t_2 = 0.0193$, $t_3 = 0.0559$ (left) and at times $t_1 = 8.5 \times 10^{-4}$, $t_2 = 5.85 \times 10^{-3}$, $t_3 = 8.85 \times 10^{-3}$ (right). The horizontal bar indicates the region $\Sigma_L(u_0)$.

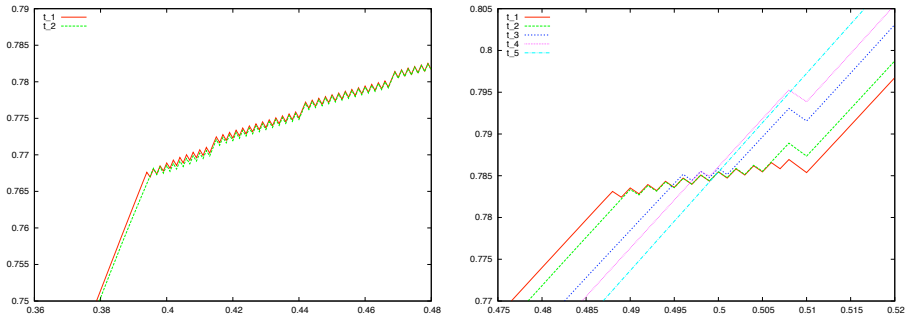

Figure 16: Test 6 (Test 2a) - Shrinking of the wrinkled region. On the left evolution at time $t_1 = 0.01$, $t_2 = 0.0103$. On the right evolution at time $t_1 = 0.0403$, $t_2 = 0.0413$, $t_3 = 0.0433$, $t_4 = 0.0443$, $t_5 = 0.0459$.

References

[1] Sigurd Angenent and Morton E. Gurtin. Multiphase thermomechanics with interfacial structure. II. Evolution of an isothermal interface. *Arch. Rational Mech. Anal.*, 108(4):323–391, 1989.

[2] Giovanni Bellettini. Anisotropic and crystalline mean curvature flow. In *A sampler of Riemann-Finsler geometry*, volume 50 of *Math. Sci. Res. Inst. Publ.*, pages 49–82. Cambridge Univ. Press, Cambridge, 2004.

[3] Giovanni Bellettini and Giorgio Fusco. The Γ-limit and the related gradient flow for singular perturbation functionals of Perona-Malik type. *Trans. Amer. Math. Soc.*, 360(9):4929–4987, 2008.

[4] Giovanni Bellettini, Giorgio Fusco, and Nicola Guglielmi. A concept of solution and numerical experiments for forward-backward diffusion equations. *Discrete Contin. Dyn. Syst.*, 16(4):783–842, 2006.

[5] Giovanni Bellettini, Carlo Mantegazza, and Matteo Novaga. Singular perturbations of mean curvature flow. *J. Differential Geom.*, 75(3):403–431, 2007.

[6] Andrea Braides. Γ-*convergence for beginners*, volume 22 of *Oxford Lecture Series in Mathematics and its Applications*. Oxford University Press, Oxford, 2002.

[7] Martin Burger, Frank Haußer, Christina Stöcker, and Axel Voigt. A level set approach to anisotropic flows with curvature regularization. *J. Comput. Phys.*, 225(1):183–205, 2007.

[8] Giuseppe Buttazzo, Mariano Giaquinta, and Stefan Hildebrandt. *One-dimensional variational problems*, volume 15 of *Oxford Lecture Series in Mathematics and its Applications*. The Clarendon Press Oxford University Press, New York, 1998. An introduction.

[9] Jack Carr, Morton E. Gurtin, and Marshall Slemrod. Structured phase transitions on a finite interval. *Arch. Rational Mech. Anal.*, 86(4):317–351, 1984.

[10] Bernard Dacorogna. *Direct methods in the calculus of variations*, volume 78 of *Applied Mathematical Sciences*. Springer, New York, second edition, 2008.

[11] Klaus Deckelnick and Gerhard Dziuk. Error analysis of a finite element method for the Willmore flow of graphs. *Interfaces Free Bound.*, 8(1):21–46, 2006.

[12] Klaus Deckelnick, Gerhard Dziuk, and Charles M. Elliott. Computation of geometric partial differential equations and mean curvature flow. *Acta Numer.*, 14:139–232, 2005.

[13] Antonio Di Carlo, Morton E. Gurtin, and Paolo Podio-Guidugli. A regularized equation for anisotropic motion-by-curvature. *SIAM J. Appl. Math.*, 52(4):1111–1119, 1992.

[14] Gerhard Dziuk. Computational parametric Willmore flow. *Numer. Math.*, 111(1):55–80, 2008.

[15] Francesca Fierro, Roberta Goglione, and Maurizio Paolini. Numerical simulations of mean curvature flow in the presence of a nonconvex anisotropy. *Math. Models Methods Appl. Sci.*, 8(4):573–601, 1998.

[16] Morton E. Gurtin. *Thermomechanics of evolving phase boundaries in the plane*. Oxford Mathematical Monographs. The Clarendon Press Oxford University Press, New York, 1993.

[17] Morton E. Gurtin and Michel E. Jabbour. Interface evolution in three dimensions with curvature-dependent energy and surface diffusion: interface-controlled evolution, phase transitions, epitaxial growth of elastic films. *Arch. Ration. Mech. Anal.*, 163(3):171–208, 2002.

[18] Morton E. Gurtin, H. Mete Soner, and Panagiotis E. Souganidis. Anisotropic motion of an interface relaxed by the formation of infinitesimal wrinkles. *J. Differential Equations*, 119(1):54–108, 1995.

[19] Frank Haußer and Axel Voigt. A numerical scheme for regularized anisotropic curve shortening flow. *Appl. Math. Lett.*, 19(8):691–698, 2006.

[20] Conyers Herring. Some theorems on the free energies of crystal surfaces. *Phys. Rev.*, 82(1):87–93, 1951.

[21] Tatiana V. Savina, Alexander A. Golovin, Stephen H. Davis, Alexander A. Nepomnyashchy, and Peter W. Voorhees. Faceting of a growing crystal surface by surface diffusion. *Phys Rev E Stat Nonlin Soft Matter Phys*, 67(2 Pt 1), 2003.

[22] Brian J. Spencer. Asymptotic solutions for the equilibrium crystal shape with small corner energy regularization. *Phys. Rev. E*, 69(1):011603, 2004.